

1 **Convergent evolution in SARS-CoV-2 Spike creates a variant soup that causes new COVID-19**  
2 **waves.**

3

4 Daniele Focosi<sup>1,#</sup>

5 Rodrigo Quiroga<sup>2</sup>

6 Scott A. McConnell<sup>3</sup>

7 Marc C Johnson<sup>4</sup>

8 Arturo Casadevall<sup>3</sup>

9

10 <sup>1</sup>North-Western Tuscany Blood Bank, Pisa University Hospital, Pisa, Italy.

11 <sup>2</sup>Instituto de Investigaciones en Físico-Química de Córdoba (INFIQC-CONICET), Facultad de Ciencias  
12 Químicas, Universidad Nacional de Córdoba, Argentina. [rquiroga@unc.edu.ar](mailto:rquiroga@unc.edu.ar)

13 <sup>3</sup>Department of Molecular Microbiology and Immunology, Johns Hopkins Bloomberg School of Public  
14 Health, Baltimore, MD, USA.

15 <sup>4</sup>Department of Molecular Microbiology and Immunology, University of Missouri School of Medicine,  
16 Columbia, MO, USA

17 #corresponding author: [daniele.focosi@gmail.com](mailto:daniele.focosi@gmail.com) .

18

19 **Word count:** abstract 177; body 3900.

20 **Author contributions:** D.F. wrote the first draft and designed Figures 3, 4, and 5; S.M. designed  
21 Figure 6, R.Q. designed Figure 4. R.Q. A.C, M.C.J.. and S.M. revised the manuscript.

22 **Keywords:** SARS-CoV-2; Spike; Omicron; convergent evolution; R346; K444; BQ.1.1; XBB; Evusheld™;  
23 cilgavimab; tixagevimab; bebtelovimab.

24 **Abbreviations:** IC: immunocompromised; MR: mutation rate; RBM : receptor-binding motif; VOC:  
25 variant of concern.

26 **Acknowledgments:** we are grateful to Cornelius Roemer (Biozentrum - Universität Basel,  
27 Switzerland), Thomas P Peacock (Imperial College, UK), independent researchers Ryan Hisner and  
28 Federico Gueli, and the Twitter user @FanDorop for discussions about convergent evolution.

29 **Abstract**

30 The first 2 years of the COVID-19 pandemic were mainly characterized by convergent evolution of  
31 mutations of SARS-CoV-2 Spike protein at residues K417, L452, E484, N501 and P681 across different  
32 variants of concern (Alpha, Beta, Gamma, and Delta). Since Spring 2022 and the third year of the  
33 pandemic, with the advent of Omicron and its sublineages, convergent evolution has led to the  
34 observation of different lineages acquiring an additional group of mutations at different amino acid  
35 residues, namely R346, K444, N450, N460, F486, F490, Q493, and S494. Mutations at these residues  
36 have become increasingly prevalent during Summer and Autumn 2022, with combinations showing  
37 increased fitness. The most likely reason for this convergence is the selective pressure exerted by  
38 previous infection- or vaccine-elicited immunity. Such accelerated evolution has caused failure of all  
39 anti-Spike monoclonal antibodies, including bebtelovimab and cilgavimab. While we are learning  
40 how fast coronaviruses can mutate and recombine, we should reconsider opportunities for  
41 economically sustainable escape-proof combination therapies, and refocus antibody-mediated  
42 therapeutic efforts on polyclonal preparations that are less likely to allow for viral immune escape.

## 43 Introduction

44 In the third year of the COVID-19 pandemic, the majority of the general population is now largely  
45 protected from severe COVID-19 disease and death by mass vaccination campaigns and by  
46 immunity from former infection. Unfortunately, SARS-CoV-2 remains a life-threatening pathogen for  
47 immunocompromised (IC) patients who are unable to mount a protective immune response. IC  
48 individuals create a cohort population in whom the virus can persistently replicate, which is a  
49 novelty for pandemics. In this regard, advancements in therapeutics and supportive care have  
50 greatly increased the prevalence of IC patients compared to just a few decades ago. SARS-CoV-2  
51 infection in IC patients is arguably the most difficult current problem in the COVID-19 pandemic for  
52 these individuals can have large viral loads with inevitably include antigenically different viruses and  
53 have a diminished capacity for clearing the infection.

54 Since Summer 2022, SARS-CoV-2 transmission has proceeded undisturbed worldwide after the  
55 relaxation of nonpharmaceutical interventions such as lockdowns, social distancing, hand hygiene,  
56 and face masks, which together with the waning of infection- and vaccine-elicited immunity, has  
57 increased opportunities for spread and the number of susceptible individuals, respectively. Hence,  
58 the increase in the “human culture medium” has led to large infectious waves during 2022, with  
59 estimated excess deaths similar to those observed in 2020 [1]. While acquisition and waning of  
60 immunity from former infections is not a novel occurrence, the COVID-19 pandemic has created  
61 conditions whereby the natural course of a coronavirus pandemic is changed by introducing timely  
62 vaccination campaigns and therapeutics targeting the viral receptor domain. There is no historical  
63 precedent for the current situation. The combined action of increasing cumulative viral loads in the  
64 “human culture medium” and such selective pressures has led to an unprecedented increase in viral  
65 diversification in 2022. WHO nomenclature for variants of concern remained stuck at “Omicron”[2],  
66 while alternative naming schemes introduced novel names to designate lineages that are  
67 responsible for thousands of hospitalizations. The most refined phylogeny to date has been released  
68 by PANGOLIN which counts more than 600 designated Omicron sublineages at the time of writing  
69 (<https://www.pango.network/summary-of-designated-omicron-lineages/>), accounting for more than  
70 45% of SARS-CoV-2 variability (Figure 1). Of interest, such increase in divergence was detected  
71 despite a 75% reduction in genomic surveillance in 2022, which is mainly due to budget constraints.  
72 After peaking at 1 million sequences in January 2022, the number of new sequences deposited at  
73 the site decreased to t 250,000 in October 2022 ([https://cov-](https://cov-spectrum.org/explore/World/AllSamples/Past6M/sequencing-coverage)  
74 [spectrum.org/explore/World/AllSamples/Past6M/sequencing-coverage](https://cov-spectrum.org/explore/World/AllSamples/Past6M/sequencing-coverage) ). Consequently, it is likely  
75 that the number of defined circulating sublineages is an underestimate of the viral genetic variation  
76 in the current pandemic.

## 77 Mutation rates and mutational spectra

78 Mutation rate (MR) is often used interchangeably to indicate 2 different things: occurrence of  
79 mutations within a single host (intrahost evolution at individual level without any demand for  
80 outcompeting co-circulating strains) or step-wise accumulation of mutations (“antigenic drift”) that  
81 get fixated within a species. While the first meaning has been demonstrated (e.g., in IC hosts[3-5],  
82 and after administration of the small molecule antiviral molnupiravir which known to increase G→A  
83 and C→U transition mutations[6], potentially contributing to new lineages), from an evolutionary  
84 standpoint it is the second meaning which is more interesting and already well-established for other  
85 respiratory pathogens[7], including the related human coronavirus 229E[8].

86 Early in the pandemic, data suggested that mass vaccination could restrict SARS-CoV-2 mutation  
87 rates (MR): the diversity of the SARS-CoV-2 lineages declined at the country-level with increased rate

88 of mass vaccination ( $r = -0.72$ ) and vaccine breakthrough patients harbor viruses with 2.3-fold lower  
89 diversity in known B cell epitopes compared to unvaccinated COVID-19 patients [9]. Also, vaccination  
90 coverage rate was inversely correlated to the MR of the SARS-CoV-2 Delta variant in 16 countries  
91 ( $r^2 = 0.878$ ) [10].

92 Ruis *et al* found a halving in the relative rate of G→T mutations in Omicron compared to pre-  
93 Omicron sublineages[11]. To exclude selective pressures on the derived protein structures, Bloom *et al*  
94 *et al* found similar results by repeating the analysis focusing on 4-fold degenerate codons (i.e. codons  
95 that can tolerate any point mutation at the third position, although codon usage bias restricts this in  
96 practice in many organisms) [12]. Replication of viruses and bacteria in the lower respiratory tract has  
97 been associated with high levels of G>T mutations and for SARS-CoV-2 this effect occurred with  
98 Delta but was lost in Omicron [11]. Such changes on mutation type and rate could theoretically stem  
99 from mutations affecting genome replication and packaging [13], as well as from mutations in  
100 genes encoding proteins (e.g. APOBEC) that antagonize host innate-immune factors, which  
101 otherwise will mutate viral nucleic acids[14-16] and/or from environmental factors [6].

102 The average MR of the entire SARS-CoV-2 genome was estimated from the related mouse hepatitis  
103 virus (MHV) to be  $10^{-6}$  nucleotides per cycle, or  $4.83 \times 10^{-4}$  subs/site/year, which is similar, or slightly  
104 lower, than observed for other RNA viruses [17]. Following the removal of mandatory  
105 nonpharmaceutical interventions such as face masks, social distancing, and quarantine in most  
106 western countries, vaccination was not sufficient to prevent hyperendemicity. The MR of SARS-CoV-  
107 2 consequently doubled from 23 substitutions per year before December 2021 to 45 substitutions  
108 per year after December 2021, coinciding with the advent of omicron (Figure 2), which approximates  
109  $14.5/\text{subs}/\text{year}$  for the  $\sim 30$  kb SARS-CoV-2 genome. This rate should set the upper limit for mutation  
110 frequency, as many mutations will not be viable and/or transmissible, and thus not observed in the  
111 sequencing data at baseline. It had been previously shown that the P203L mutation in the error-  
112 correcting exonuclease non-structural protein 14 (nsp14) almost doubles the genomic MR (from 20  
113 to 36 SNPs/year) [18]. While this change is not prevalent in Omicron lineages, many changes in the  
114 replication machinery appeared with Omicron, such as K38R,  $\Delta 1265$ , and A1892T in Nsp3; P132H in  
115 Nsp5; I189V in Nsp6; P323L in Nsp12; and I42V in Nsp14, and some of them could have contributed  
116 to the MR jump[19].

## 117 Convergent evolution

118 In the midst of such massive lineage divergence, convergent evolution towards certain motifs has  
119 become increasingly manifest.

120 In the pre-Omicron and pre-vaccine era, variants of concern (VOCs) notably converged to mutations  
121 which resulted in the following amino acid changes: K417N, L452R, E484K, N501Y, and P681X[20].  
122 These amino acid changes have been proposed to increase the stability of the trimeric protein[21-  
123 23], and they emerged in the absence of significant selective pressures by the immune system.  
124 K417N, E484A, N501Y and P681H remained hallmarks of BA.2.\*, while the paraphyletic BA.4/5  
125 acquired L452R and F486V and the Q493R reversion.

126 In the last year the BA.2 variant first generated a wave that led first to the paraphyletic BA.4/5  
127 sublineage, which was later joined by a return of so-called “second-generation” BA.2 sublineages  
128 (Figure 3), with BA.2.75.\* and BA.2.3.20 being the most circulated. Since Summer 2022, each of  
129 those sublineages has amazingly converged with changes at the receptor-binding domain (RBD)  
130 residues R346, K444, L452, N450, N460, F486, F490, Q493, and S494 (see Supplementary Table  
131 1)[24]. E484A remained instead stable, with E484K never detected, A484G seen only in BA.2.3.20, and

132 A484T seen only in XBB.1.3. More recently, convergence in indels within the N-terminal domain  
133 (NTD), as previously recognized in Brazilian VOCs[25], was reported for Omicron sublineages: in  
134 particular, Y144del has been found in BA.4.6.3, BJ.1, BU.1, BQ.1.8.\*, BQ.1.1.10, BQ.1.1.20, BQ.1.18,  
135 and XBB.\*)[26].

136 This “variant soup” can be organized and stratified according to the number of key Spike mutations  
137 present, and although the number of key mutations acquired correlates well with increasing fitness,  
138 this is only so within each lineage, which shows that the biology of SARS-COV-2 infection goes  
139 beyond what occurs in the Spike protein (Figure 4). At present, only the BQ.1-derived lineages with 7  
140 or more selected mutations display a clear relative growth advantage relative comparison to the  
141 BQ.1.1 baseline. Convergence was clearly observed at the amino acid level, with different nucleotide  
142 mutations leading to similar amino acid changes: e.g., N460K was caused by T22942A in BQ.1\*, XAW  
143 and some of the BA.5.2 sublineages, while it was caused by T22942G in BA.2.75\*(all lineages),  
144 BA.2.3.20, BS.1, BU.1, XBB, XAK and BW.1 (BA.5.6.2.1). Another impressive example of this  
145 convergent evolution is the Spike of BA.4.6.3, BQ.1.18 and BQ.1.1.20 independently acquiring the  
146 following amino acid changes since their last shared common ancestor: Y144del, R346T, N460K,  
147 L452R, F486V and the R493Q reversion. Also, BA.4.6.3 has acquired K444N, while BQ.1.18 and  
148 BQ.1.1.20 acquired K444T.

## 149 Escalating immune escape

150 SARS-CoV-2 evolution represents an accelerated movie of Darwinian selection. Variants that are  
151 more likely to escape vaccine- and infection-elicited immunity that are more fit expand at the  
152 expense of those less fit. While it may sound obvious, we now have formal evidence of such  
153 evolution, with PANGOLIN descendants invariably having increased RBD immune escape scores  
154 compared to parental strains (Figure 5). In this ongoing race, descendants invariably replace parents,  
155 as these are fitter in hosts with pre-existing immunity. In this regard, the chances for saltations  
156 lineages that emerged after intrahost evolution in IC patients (i.e. in the absence of RBD immune  
157 escape) seem minimal: accordingly, despite the initial hypothesis of intrahost evolution to explain  
158 the saltation seen with the emergence of Omicron, recent evidence suggests that Omicron  
159 ancestors circulated undetected long before the exponential spread [27].

160 RBD immune escape can nowadays be estimated *in silico* based on *in vitro* data  
161 ([https://jbloomlab.github.io/SARS2\\_RBD\\_Ab\\_escape\\_maps/escape-calc/](https://jbloomlab.github.io/SARS2_RBD_Ab_escape_maps/escape-calc/)). RBD immune escape is  
162 clearly a moving scale with an evolving asymptote. E.g., by changing vaccine composition [28] we are  
163 likely to reset the “game”.

164

## 165 ACE2 affinity fine tuning

166 ACE2 affinity can be estimated *in silico* ([https://github.com/jbloomlab/SARS-CoV-2-  
167 RBD\\_DMS\\_Omicron/blob/main/results/final\\_variant\\_scores/final\\_variant\\_scores.csv](https://github.com/jbloomlab/SARS-CoV-2-RBD_DMS_Omicron/blob/main/results/final_variant_scores/final_variant_scores.csv)). Several  
168 Omicron sublineages showed remarkable examples of further evolution at Spike residues that were  
169 already recently mutated. E.g.,

- 170 • BQ.1 already had K444T inherited from BE.1.1.1, but further mutated into 444M in the child  
171 BQ.1.1.17
- 172 • XBB.1 already had E484A inherited from the BA.2 parent, but further mutated into 484T in  
173 the child XBB.1.3

- 174       • BA.2.3 already had E484A inherited from the BA.2 parent, but further mutated into 484G in  
175       the child BA.2.3.20, which caused an impressive increase in ACE2 affinity (to whom K444R,  
176       L452M, and N460K contributed)
- 177       • BM.4.1.1 already had F486S inherited from the BM.4.1 parent but further mutated into  
178       486P in CH.3
- 179       • BM.1.1.1 already had F486S inherited from the BM.1 parent but further mutated into 486P  
180       in the child CJ.1
- 181       • XBB.1 already had F486S inherited from the BM.1.1.1 parent but further mutated into 486P  
182       in the child XBB.1.5
- 183       • BA.2.75.2 already had F486S inherited from the BA.2.75 parent, but further mutated into  
184       486L in the child CA.4
- 185       • BA.5.2.1 already had F486V inherited since BA.5, but further mutated to 486I in BF.12
- 186       • BW.1 already had F486V inherited from the BA.5 parent, but further mutated into 486S in  
187       the child BW.1.1
- 188       Seven of these examples manifest escalating affinities for ACE2, with the other 2 representing no  
189       change in ACE2 affinity (**Figure 6**).

190

## 191 Mutually exclusive mutations

192 Mutually exclusive mutations across the entire SARS-CoV-2 genome have been previously  
193 studied[29], but the vast constellation of Omicron sublineages provides an unique opportunity for an  
194 in-depth exploration of substitutions that are incompatible in combination. The best examples so far  
195 are N450X and R346X mutations, which have not yet been observed together in more than 6 millions  
196 of Omicron sequences. Two dipolar interactions exist between the carboxamide group of Asn and  
197 the guanidino group of Arg in the ancestral sequence, stabilizing the receptor binding module (RBM)  
198 tertiary fold (Figure 7, left). R346 resides within a short loop between helix  $\alpha$ 1 and beta strand 1.  
199 N450 is a constituent of the extended RBM insertion into the overall five-stranded antiparallel beta-  
200 sheet fold of the domain. As the RBM is the critical determinant for the interaction with ACE2,  
201 maintaining its optimal conformation through this stabilizing bond is likely to be essential for  
202 pathogenesis. N450D is a common substitution among Omicron lineages. This mutation would result  
203 in a similarly sized sidechain but different electrostatic properties (carboxamine  $\rightarrow$  carboxylic acid).  
204 This substitution would likely result in a stronger interaction with position 450, as one H-bonding is  
205 maintained, and one is replaced with ionic salt bridge between the deprotonated oxygen and the  
206 basic guanidino group, provided that the residue at position 346 remains Arg. On the other hand,  
207 any substitution at position 346, with the exception of Lys, would result in a significantly shorter,  
208 non-cationic sidechain, which would abrogate this RBM-stabilizing interaction. R346K would partially  
209 maintain this interaction, replacing a bidentate linkage to N450 with a monodentate dipolar  
210 interaction. Thus, the observed mutual exclusivity of mutations at these two sites can be rationalized  
211 by their contributions to this stabilizing intradomain interaction.

212 Other combinations have been exceedingly rare so far, and seen only in cryptic lineages (e.g., F486P  
213 and K444 mutations), but no steric justifications can be found for them.

## 214 Epistasis

215 While the focus so far has been mostly on the Spike protein, it is likely that convergent evolution is  
216 acting on genes other than Spike. Given that the Spike protein is the best protective antigen for both

217 infection and vaccines, mutations in other genes are more likely to provide fitness advantages if they  
218 affect Spike expression. E.g., ORF8 limits the amount of Spike proteins that reaches the cell surface  
219 and is incorporated into virions, reducing recognition by anti-SARS-CoV-2 antibodies[30]. ORF8 has  
220 accordingly been target of convergent evolution in Omicron (e.g., ORF8:S667F in BR.2.1, ORF8:G8x in  
221 XBB.1) and in SARS-related coronaviruses[31].

222 Other genes whose roles in Spike modulation are not clear are also converging, such as  
223 ORF1b:T1050, found in many BA.5.2.\* sublineages, and XBE (T1050N) as well as XBC.\* (T1050I).

224

## 225 **Selective pressures from therapeutics targeting the Spike** 226 **protein.**

227 There is a theoretical concern that, in addition to vaccines- and infection-elicited immunity, selective  
228 pressure by prophylactic and therapeutic anti-Spike monoclonal antibodies (mAb), can contribute to  
229 the emergence of novel SARS-CoV-2 sublineages [32]. While selective pressures are likely to generate  
230 many different mutants, a very few of those emerging sublineages could be fit enough to compete  
231 with the lineages that are dominating at that time to become locally or globally dominant.

232 While spontaneous evolution can occur in the absence of selective pressures due to the intrinsic  
233 genomic MR (see section above), extended half-life mAbs (such as Evusheld™) administered for pre-  
234 exposure prophylaxis or therapy to chronically infected immunocompromised patients at  
235 subneutralizing concentrations provide ideal conditions to facilitate the emergence of mutants[33],  
236 for these patients often cannot clear the infection and have high viral loads. Establishing a cause-  
237 effect relationship is difficult, but intra-host evolution studies provide a highly suggestive temporal  
238 association[34]. mAbs have come of age since the advent of the SARS-CoV-2 Delta VOC, but because  
239 of the resistance of Omicron to most authorized mAbs, their use since Spring 2022 has been largely  
240 limited to Evusheld™ (for which cilgavimab was the only ingredient with residual activity) and  
241 bebtelovimab.

242 We know from *in vitro* deep mutational scanning studies the exact mutations that cause resistance  
243 to each mAb. S:F486X mutations impart resistance to tixagevimab, S:R346X, S:K444X and S:S494X  
244 mutations impart resistance to cilgavimab, while S:K444X mutations impart resistance to  
245 bebtelovimab (Table 1). We recently noted an increase in the circulation of Omicron sublineages  
246 associated with S:R346X mutations, and wondered whether this could partly be the result of  
247 selective pressure with Evusheld™. We compared the prevalence of R346X mutations in countries  
248 with high versus low usage of Evusheld™ (France vs. UK) or bebtelovimab (USA vs. UK) (Figure 8). UK  
249 also represents an ideal control because of its very high SARS-CoV-2 genome sequencing rate. We  
250 discuss these 2 scenarios in details below.

251

### 252 **S:R346X**

253 Different mutations can affect the R346 residue. R346G has been selected *in vitro* by  
254 cilgavimab+tixagevimab[35]. R346S occurred *in vitro* after 12 weeks of propagating SARS-CoV-2 in  
255 the presence of sotrovimab, and before the other epitope mutation (P337L) which leads to  
256 sotrovimab resistance [36]. R346I has been selected *in vitro* under the selective pressure from  
257 cilgavimab [37,38]. Lee *et al* reported mutually exclusive substitutions at residues R346 (R346S and  
258 R346I) and E484 (E484K and E484A) of Spike protein and continuous turnover of these substitutions  
259 in 2 immunosuppressed patients[39]. Unfortunately, *in vivo* selection evidences are so far available

260 for sotrovimab[40] but not for Evusheld™. It should be anyway noted that R346T[41,42] and R346I[43]  
261 have been reported to spontaneously develop and fix in 3 IC patients without any selective pressure.

262 While R346K was associated with the BA.1.1 wave (see Figure 8), the plethora of different Omicron  
263 sublineages that showed convergent evolution towards R346I, R346S or R346T is of concern.

- 264 • R346K (previously seen only in VOC Mu/B.1.621 [44]) occurred exclusively in BA.1.1, a  
265 sublineage that disappeared since May 2022, where it affected the interaction network in  
266 the BA.1.1 RBD/hACE2 interface through long-range alterations and contributes to the  
267 higher hACE2 affinity of the BA.1.1 RBD than the BA.1 RBD [45], and had increased resistance  
268 against Evusheld™[46] and sotrovimab[47]. Only STI-9167 remained effective among the  
269 mAbs[48]. Beta+R346K, which was identified in the Philippines in August 2021, exhibited the  
270 highest resistance to 2 BNT61b2 doses-elicited sera among the tested VOCs[49]. After  
271 BA.1.1, R346K has not been detected worldwide in any sublineage.
- 272 • R346I occurs in more than 40 different Omicron sublineages, but it is most represented in  
273 BA.5.9 (38%), BA.4.1 (5%), BA.5.9 (4%), but also occurred in AY.39 (14%);
- 274 • R346S (previously seen only in a C.36.3 sublineage from Italy[50] (30.8%), occurs in more  
275 than 40 different Omicron sublineages but it is most represented in B.1.640.1 (18%), and in a  
276 few Delta sublineages (<2%) occurs nowadays in BA.4.7 (13%), BA.5.2.1 (8.22%), BA.4  
277 (2.8%).
- 278 • R346T occurs in more than 96 different Omicron sublineages, but it is mostly represented in  
279 BA.4.6 (44%), BA.5.2.1 (13%), BA.2 (8%), BA.2.74 (3%), BA.2.76 (12%), BA.4.1 (2.3%). In  
280 addition, it is a hallmark mutation of BA.1.23, BA.2.9.4, BL.1, BA.2.75.2, BA.2.80, BA.2.82,  
281 BA.4.1.8, BF.7 and BF.11. BA.4.6, BA.4.7, and BA.5.9 displayed higher humoral immunity  
282 evasion capability than BA.4/BA.5, causing 1.5 to 1.9-fold decrease in NT<sub>50</sub> of the plasma  
283 from BA.1 and BA.2 breakthrough-infection convalescents compared to BA.4/BA.5.  
284 Importantly, plasma from BA.5 breakthrough-infection convalescents also exhibits significant  
285 neutralization activity decrease against BA.4.6, BA.4.7, and BA.5.9 than BA.4/BA.5, showing  
286 on average 2.4 to 2.6-fold decrease in NT<sub>50</sub>. R346S causes resistance to class 3 antibodies:  
287 bebtelovimab remains potent, while Evusheld™ is completely escaped by these subvariants  
288 [51].

289

## 290 S:K444X

291 The K444E/R mutations were reported *in vitro* after selection with cilgavimab[38]. Resistance studies  
292 with bebtelovimab selected the K444T escape mutations for BA.2[52]. Ortega *et al* found that K444R  
293 (previously found in the Beta VOC[53]), K444Q, and K444N mutations can change the virus binding  
294 affinity to the ACE2 receptor[54]. Weisblum *et al* found that K444R/Q/N occurs after exposure to  
295 convalescent plasma[55]. Among largely diversified VOCs such as Delta, S:K444N was associated with  
296 reduced remdesivir binding and increased mortality[56].

297

## 298 Conclusions

299 The convergent evolution of Omicron sublineages appears to reflect the selective pressure exerted  
300 by previous infection- or vaccine-elicited immunity. Vaccines and perhaps antibody therapeutics  
301 have without doubt saved an untold number of lives but also likely altered the natural evolutionary  
302 trajectory of the virus. While other viruses such as influenza and HIV routinely produced new  
303 variants because of their mutagenicity, the scale at which SARS-CoV-2 has spun off new variants and



304 lineages appears unprecedented in modern virology history. The SARS-CoV-2 vaccines reduce severe  
305 disease and mortality but do not confer sufficient immunity to prevent re-infection with viral  
306 replication in vaccinated hosts. Hence, we have the unusual situation of viral replication in immune  
307 hosts where the immune system is placing evolutionary pressure on the virus to select variants that  
308 can escape vaccine-elicited immunity in addition to infection-elicited immunity. Whether this rapid  
309 evolutionary trajectory is the result of viral replication properties, replication in immune hosts or  
310 both is unknown but conditions present in the past year of the pandemic have produced a  
311 remarkable natural experiment in viral evolution for which we cannot discern its conclusion.

312 Insights from structural biology has shown how some mutations are mutually exclusive, which could  
313 help the design of next-generation vaccines. But the latter could reset the run for immune escape,  
314 perpetuating the never-ending game of host and pathogen. Viral recombination[57] (more than 50  
315 lineages censused at the time of writing, with both simple and complex variants[58]) and sudden  
316 reemergence of former VOCs[59] have to be considered as further drivers for evolutionary saltation.

317 In this setting, polyclonal passive immunotherapies (such as plasma from convalescent and  
318 vaccinated donors[60,61]) appear more escape-resistant than monoclonal antibodies[62-65], and  
319 combo therapies should be urgently investigated and deployed in vulnerable populations, such as IC  
320 patients[66].

321

## 322 References

- 323 1. Daily new confirmed COVID-19 deaths per million people. Our world in data. Accessed online  
324 at [https://ourworldindata.org/explorers/coronavirus-data-  
325 explorer?zoomToSelection=true&time=2020-03-  
326 01..latest&facet=none&pickerSort=asc&pickerMetric=location&hideControls=false&Metric=  
327 Confirmed+deaths&Interval=7-  
328 day+rolling+average&Relative+to+Population=true&Color+by+test+positivity=false&country  
329 =~OWID\\_WRL](https://ourworldindata.org/explorers/coronavirus-data-explorer?zoomToSelection=true&time=2020-03-01..latest&facet=none&pickerSort=asc&pickerMetric=location&hideControls=false&Metric=Confirmed+deaths&Interval=7-day+rolling+average&Relative+to+Population=true&Color+by+test+positivity=false&country=~OWID_WRL) on December 1, 2022.
- 330 2. Viana, R.; Moyo, S.; Amoako, D.G.; Tegally, H.; Scheepers, C.; Althaus, C.L.; Anyaneji, U.J.;  
331 Bester, P.A.; Boni, M.F.; Chand, M.; et al. Rapid epidemic expansion of the SARS-CoV-2  
332 Omicron variant in southern Africa. *Nature* **2022**, *603*, 679-686, doi:10.1038/s41586-022-  
333 04411-y.
- 334 3. Harari, S.; Tahor, M.; Rutsinsky, N.; Meijer, S.; Miller, D.; Henig, O.; Halutz, O.; Levytskyi, K.;  
335 Ben-Ami, R.; Adler, A.; et al. Drivers of adaptive evolution during chronic SARS-CoV-2  
336 infections. *Nat Med* **2022**, *28*, 1501-1508, doi:10.1038/s41591-022-01882-4.
- 337 4. Kemp, S.A.; Collier, D.A.; Datir, R.P.; Ferreira, I.A.T.M.; Gayed, S.; Jahun, A.; Hosmillo, M.;  
338 Rees-Spear, C.; Mlcochova, P.; Lumb, I.U.; et al. SARS-CoV-2 evolution during treatment of  
339 chronic infection. *Nature* **2021**, *592*, 277-282, doi:10.1038/s41586-021-03291-y.
- 340 5. Wilkinson, S.A.J.; Richter, A.; Casey, A.; Osman, H.; Mirza, J.D.; Stockton, J.; Quick, J.;  
341 Ratcliffe, L.; Sparks, N.; Cumley, N.; et al. Recurrent SARS-CoV-2 mutations in  
342 immunodeficient patients. *Virus Evol* **2022**, *8*, veac050, doi:10.1093/ve/veac050.
- 343 6. Focosi, D. Molnupiravir: From Hope to Epic Fail? **2022**, *14*, 2560.
- 344 7. Smith, D.J.; Lapedes, A.S.; de Jong, J.C.; Bestebroer, T.M.; Rimmelzwaan, G.F.; Osterhaus,  
345 A.D.; Fouchier, R.A. Mapping the antigenic and genetic evolution of influenza virus. *Science*  
346 **2004**, *305*, 371-376, doi:10.1126/science.1097211.
- 347 8. Eguia, R.T.; Crawford, K.H.D.; Stevens-Ayers, T.; Kelnhofer-Millevolte, L.; Greninger, A.L.;  
348 Englund, J.A.; Boeckh, M.J.; Bloom, J.D. A human coronavirus evolves antigenically to escape  
349 antibody immunity. *PLoS Pathog* **2021**, *17*, e1009453, doi:10.1371/journal.ppat.1009453.

- 350 9. Niesen, M.; Anand, P.; Silvert, E.; Suratekar, R.; Pawlowski, C.; Ghosh, P.; Lenehan, P.;  
351 Hughes, T.; Zemmour, D.; OHoro, J.C.; et al. COVID-19 vaccines dampen genomic diversity of  
352 SARS-CoV-2: Unvaccinated patients exhibit more antigenic mutational variance. **2021**,  
353 2021.2007.2001.21259833, doi:10.1101/2021.07.01.21259833 %J medRxiv.
- 354 10. Yeh, T.-Y.; Contreras, G.P. Full vaccination is imperative to suppress SARS-CoV-2 delta variant  
355 mutation frequency. **2021**, 2021.2008.2008.21261768, doi:10.1101/2021.08.08.21261768  
356 %J medRxiv.
- 357 11. Ruis, C.; Peacock, T.P.; Polo, L.M.; Masone, D.; Alvarez, M.S.; Hinrichs, A.S.; Turakhia, Y.;  
358 Cheng, Y.; McBroom, J.; Corbett-Detig, R.; et al. Mutational spectra distinguish SARS-CoV-2  
359 replication niches. **2022**, 2022.2009.2027.509649, doi:10.1101/2022.09.27.509649 %J  
360 bioRxiv.
- 361 12. Bloom, J.D.; Beichman, A.C.; Neher, R.A.; Harris, K. Evolution of the SARS-CoV-2 mutational  
362 spectrum. **2022**, 2022.2011.2019.517207, doi:10.1101/2022.11.19.517207 %J bioRxiv.
- 363 13. V'Kovski, P.; Kratzel, A.; Steiner, S.; Stalder, H.; Thiel, V. Coronavirus biology and replication:  
364 implications for SARS-CoV-2. *Nature reviews. Microbiology* **2021**, *19*, 155-170,  
365 doi:10.1038/s41579-020-00468-6.
- 366 14. Sadler, H.A.; Stenglein, M.D.; Harris, R.S.; Mansky, L.M. APOBEC3G contributes to HIV-1  
367 variation through sublethal mutagenesis. *Journal of virology* **2010**, *84*, 7396-7404,  
368 doi:10.1128/jvi.00056-10.
- 369 15. De Maio, N.; Walker, C.R.; Turakhia, Y.; Lanfear, R.; Corbett-Detig, R.; Goldman, N. Mutation  
370 Rates and Selection on Synonymous Mutations in SARS-CoV-2. *Genome biology and*  
371 *evolution* **2021**, *13*, doi:10.1093/gbe/evab087.
- 372 16. Ratcliff, J.; Simmonds, P. Potential APOBEC-mediated RNA editing of the genomes of SARS-  
373 CoV-2 and other coronaviruses and its impact on their longer term evolution. *Virology* **2021**,  
374 *556*, 62-72, doi:10.1016/j.virol.2020.12.018.
- 375 17. Mercatelli, D.; Giorgi, F.M. Geographic and Genomic Distribution of SARS-CoV-2 Mutations.  
376 **2020**, *11*, doi:10.3389/fmicb.2020.01800.
- 377 18. Takada, K.; Ueda, M.T.; Watanabe, T.; Nakagawa, S. Genomic diversity of SARS-CoV-2 can be  
378 accelerated by a mutation in the nsp14 gene. **2020**, 2020.2012.2023.424231,  
379 doi:10.1101/2020.12.23.424231 %J bioRxiv.
- 380 19. Jung, C.; Kmiec, D.; Koepke, L.; Zech, F.; Jacob, T.; Sparrer, K.M.J.; Kirchhoff, F. Omicron:  
381 What Makes the Latest SARS-CoV-2 Variant of Concern So Concerning? **2022**, *96*, e02077-  
382 02021, doi:doi:10.1128/jvi.02077-21.
- 383 20. Focosi, D. *SARS-CoV-2 Spike protein convergent evolution* 2021.
- 384 21. Neto, D.F.L.; Fonseca, V.; Jesus, R.; Dutra, L.H.; Portela, L.M.O.; Freitas, C.; Fillizola, E.;  
385 Soares, B.; Abreu, A.L.; Twiari, S.; et al. Molecular dynamics simulations of the SARS-CoV-2  
386 Spike protein and variants of concern: structural evidence for convergent adaptive  
387 evolution. *Journal of biomolecular structure & dynamics* **2022**, 1-13,  
388 doi:10.1080/07391102.2022.2097955.
- 389 22. Upadhyay, V.; Patrick, C.; Lucas, A.; Mallela, K.M.G. Convergent Evolution of Multiple  
390 Mutations Improves the Viral Fitness of SARS-CoV-2 Variants by Balancing Positive and  
391 Negative Selection. *Biochemistry* **2022**, *61*, 963-980, doi:10.1021/acs.biochem.2c00132.
- 392 23. Martin, D.P.; Weaver, S.; Tegally, H.; San, J.E.; Shank, S.D.; Wilkinson, E.; Lucaci, A.G.;  
393 Giandhari, J.; Naidoo, S.; Pillay, Y.; et al. The emergence and ongoing convergent evolution of  
394 the SARS-CoV-2 N501Y lineages. *Cell* **2021**, *184*, 5189-5200.e5187,  
395 doi:10.1016/j.cell.2021.09.003.
- 396 24. Variant report 2022-09-14. Accessed online at [https://github.com/neherlab/SARS-CoV-](https://github.com/neherlab/SARS-CoV-2_variant-reports/blob/main/reports/variant_report_2022-09-14.md)  
397 [2\\_variant-reports/blob/main/reports/variant\\_report\\_2022-09-14.md](https://github.com/neherlab/SARS-CoV-2_variant-reports/blob/main/reports/variant_report_2022-09-14.md) on November 23,  
398 2022.
- 399 25. Resende, P.C.; Naveca, F.G.; Lins, R.D.; Dezordi, F.Z.; Ferraz, M.V.F.; Moreira, E.G.; Coêlho,  
400 D.F.; Motta, F.C.; Paixão, A.C.D.; Appolinario, L.; et al. The ongoing evolution of variants of

- 401 concern and interest of SARS-CoV-2 in Brazil revealed by convergent indels in the amino (N)-  
402 terminal domain of the spike protein. *Virus Evol* **2021**, *7*, veab069, doi:10.1093/ve/veab069.
- 403 26. Cao, Y.; Jian, F.; Wang, J.; Yu, Y.; Song, W.; Yisimayi, A.; Wang, J.; An, R.; Zhang, N.; Wang, Y.;  
404 et al. Imprinted SARS-CoV-2 humoral immunity induces convergent Omicron RBD evolution.  
405 **2022**, 2022.2009.2015.507787, doi:10.1101/2022.09.15.507787 %J bioRxiv.
- 406 27. Fischer, C.; Maponga, T.G.; Yadouleton, A.; Abílio, N.; Aboce, E.; Adewumi, P.; Afonso, P.;  
407 Akorli, J.; Andriamandimby, S.F.; Anga, L.; et al. Gradual emergence followed by exponential  
408 spread of the SARS-CoV-2 Omicron variant in Africa. *O*, eadd8737,  
409 doi:doi:10.1126/science.add8737.
- 410 28. Focosi, D.; Maggi, F. Do We Really Need Omicron Spike-Based Updated COVID-19 Vaccines?  
411 Evidence and Pipeline. *Viruses* **2022**, *14*, doi:10.3390/v14112488.
- 412 29. Al Khalaf, R.; Bernasconi, A.; Pinoli, P.; Ceri, S. Analysis of co-occurring and mutually exclusive  
413 amino acid changes and detection of convergent and divergent evolution events in SARS-  
414 CoV-2. *Computational and structural biotechnology journal* **2022**, *20*, 4238-4250,  
415 doi:10.1016/j.csbj.2022.07.051.
- 416 30. Kim, I.-J.; Lee, Y.-h.; Khalid, M.M.; Zhang, Y.; Ott, M.; Verdin, E. SARS-CoV-2 ORF8 limits  
417 expression levels of Spike antigen. **2022**, 2022.2011.2009.515752,  
418 doi:10.1101/2022.11.09.515752 %J bioRxiv.
- 419 31. Akaishi, T.; Fujiwara, K.; Ishii, T. Insertion/deletion hotspots in the Nsp2, Nsp3, S1, and ORF8  
420 genes of SARS-related coronaviruses. *BMC ecology and evolution* **2022**, *22*, 123,  
421 doi:10.1186/s12862-022-02078-7.
- 422 32. Focosi, D.; McConnell, S.; Casadevall, A.; Cappello, E.; Valdiserra, G.; Tuccori, M. Monoclonal  
423 antibody therapies against SARS-CoV-2. *The Lancet Infectious Diseases* **2022**, *22*, 00311-  
424 00315, doi:10.1016/S1473-3099(22)00311-5.
- 425 33. Focosi, D.; Casadevall, A. A Critical Analysis of the Use of Cilgavimab plus Tixagevimab  
426 Monoclonal Antibody Cocktail (Evusheld&trade;) for COVID19 Prophylaxis and Treatment.  
427 **2022**, *14*, 1999.
- 428 34. Focosi, D.; Maggi, F.; Franchini, M.; McConnell, S.; Casadevall, A. Analysis of Immune Escape  
429 Variants from Antibody-Based Therapeutics against COVID-19: A Systematic Review.  
430 *International journal of molecular sciences* **2022**, *23*, 29.
- 431 35. Copin, R.; Baum, A.; Wloga, E.; Pascal, K.E.; Giordano, S.; Fulton, B.O.; Zhou, A.; Negron, N.;  
432 Lanza, K.; Chan, N.; et al. The monoclonal antibody combination REGEN-COV protects  
433 against SARS-CoV-2 mutational escape in preclinical and human studies. *Cell* **2021**, *184*,  
434 3949-3961, doi: 10.1016/j.cell.2021.06.002.
- 435 36. Magnus, C.L.; Hiergeist, A.; Schuster, P.; Rohrhofer, A.; Medenbach, J.; Gessner, A.;  
436 Peterhoff, D.; Schmidt, B. Targeted escape of SARS-CoV-2 in vitro from monoclonal antibody  
437 S309, the precursor of sotrovimab. *Frontiers in immunology* **2022**, *13*, 966236,  
438 doi:10.3389/fimmu.2022.966236.
- 439 37. Dong, J.; Zost, S.J.; Greaney, A.J.; Starr, T.N.; Dingens, A.S.; Chen, E.C.; Chen, R.E.; Case, J.B.;  
440 Sutton, R.E.; Gilchuk, P.; et al. Genetic and structural basis for SARS-CoV-2 variant  
441 neutralization by a two-antibody cocktail. *Nat Microbiol* **2021**, *6*, 1233-1244,  
442 doi:10.1038/s41564-021-00972-2.
- 443 38. FDA. Fact sheet for healthcare providers: emergency use authorization for Evusheld™  
444 (tixagevimab co-packaged with cilgavimab). Accessed online at  
445 <https://www.fda.gov/media/154701/download> on August 13, 2022. **2021**.
- 446 39. Lee, J.S.; Yun, K.W.; Jeong, H.; Kim, B.; Kim, M.J.; Park, J.H.; Shin, H.S.; Oh, H.S.; Sung, H.;  
447 Song, M.G.; et al. SARS-CoV-2 shedding dynamics and transmission in immunosuppressed  
448 patients. *Virulence* **2022**, *13*, 1242-1251, doi:10.1080/21505594.2022.2101198.
- 449 40. Andrés, C.; González-Sánchez, A.; Jiménez, M.; Márquez-Algaba, E.; Piñana, M.; Fernández-  
450 Naval, C.; Esperalba, J.; Saubi, N.; Quer, J.; Rando-Segura, A.; et al. Emergence of Delta and  
451 Omicron variants carrying resistance-associated mutations in immunocompromised patients

- 452 undergoing Sotrovimab treatment with long viral excretion. *Clinical microbiology and*  
453 *infection : the official publication of the European Society of Clinical Microbiology and*  
454 *Infectious Diseases* **2022**, doi:10.1016/j.cmi.2022.08.021.
- 455 41. Gonzalez-Reiche, A.S.; Alshammary, H.; Schaefer, S.; Patel, G.; Polanco, J.; Amoako, A.A.;  
456 Rooker, A.; Cognigni, C.; Floda, D.; van de Guchte, A.; et al. Intrahost evolution and forward  
457 transmission of a novel SARS-CoV-2 Omicron BA.1 subvariant. **2022**,  
458 2022.2005.2025.22275533, doi:10.1101/2022.05.25.22275533 %J medRxiv.
- 459 42. Lee, C.Y.; Shah, M.K.; Hoyos, D.; Solovyov, A.; Douglas, M.; Taur, Y.; Maslak, P.; Babady, N.E.;  
460 Greenbaum, B.; Kamboj, M.; et al. Prolonged SARS-CoV-2 Infection in Patients with  
461 Lymphoid Malignancies. *Cancer discovery* **2022**, *12*, 62-73, doi:10.1158/2159-8290.Cd-21-  
462 1033.
- 463 43. Sonnleitner, S.T.; Prelog, M.; Sonnleitner, S.; Hinterbichler, E.; Halbfurter, H.; Kopecky,  
464 D.B.C.; Almanzar, G.; Koblmüller, S.; Sturmbauer, C.; Feist, L.; et al. Cumulative SARS-CoV-2  
465 mutations and corresponding changes in immunity in an immunocompromised patient  
466 indicate viral evolution within the host. *Nat Commun* **2022**, *13*, 2560, doi:10.1038/s41467-  
467 022-30163-4.
- 468 44. Fratev, F. R346K Mutation in the Mu Variant of SARS-CoV-2 Alters the Interactions with  
469 Monoclonal Antibodies from Class 2: A Free Energy Perturbation Study. *Journal of chemical*  
470 *information and modeling* **2022**, *62*, 627-631, doi:10.1021/acs.jcim.1c01243.
- 471 45. Li, L.; Liao, H.; Meng, Y.; Li, W.; Han, P.; Liu, K.; Wang, Q.; Li, D.; Zhang, Y.; Wang, L.; et al.  
472 Structural basis of human ACE2 higher binding affinity to currently circulating Omicron SARS-  
473 CoV-2 sub-variants BA.2 and BA.1.1. *Cell* **2022**, *185*, 2952-2960.e2910,  
474 doi:10.1016/j.cell.2022.06.023.
- 475 46. Uraki, R.; Kiso, M.; Imai, M.; Yamayoshi, S.; Ito, M.; Fujisaki, S.; Takashita, E.; Ujie, M.;  
476 Furusawa, Y.; Yasuhara, A.; et al. Therapeutic efficacy of monoclonal antibodies and  
477 antivirals against SARS-CoV-2 Omicron BA.1 in Syrian hamsters. *Nat Microbiol* **2022**, *7*, 1252-  
478 1258, doi:10.1038/s41564-022-01170-4.
- 479 47. Nutalai, R.; Zhou, D.; Tuekprakhon, A.; Ginn, H.M.; Supasa, P.; Liu, C.; Huo, J.; Mentzer, A.J.;  
480 Duyvesteyn, H.M.E.; Djokaite-Guraliuc, A.; et al. Potent cross-reactive antibodies following  
481 Omicron breakthrough in vaccinees. *Cell* **2022**, *185*, 2116-2131.e2118,  
482 doi:10.1016/j.cell.2022.05.014.
- 483 48. Duty, J.A.; Kraus, T.; Zhou, H.; Zhang, Y.; Shaabani, N.; Yildiz, S.; Du, N.; Singh, A.; Miorin, L.;  
484 Li, D.; et al. Discovery of a SARS-CoV-2 Broadly-Acting Neutralizing Antibody with Activity  
485 against Omicron and Omicron + R346K Variants. **2022**, 2022.2001.2019.476998,  
486 doi:10.1101/2022.01.19.476998 %J bioRxiv.
- 487 49. Koyama, T.; Miyakawa, K.; Tokumasu, R.; S, S.J.; Kudo, M.; Ryo, A. Evasion of vaccine-induced  
488 humoral immunity by emerging sub-variants of SARS-CoV-2. *Future microbiology* **2022**, *17*,  
489 417-424, doi:10.2217/fmb-2022-0025.
- 490 50. Castelli, M.; Baj, A.; Criscuolo, E.; Ferrarese, R.; Diotti, R.; Sampaolo, M.; Novazzi, F.; Dalla  
491 Gasperina, D.; Focosi, D.; Locatelli, M.; et al. Characterization of a lineage C.36 SARS-CoV-2  
492 isolate with reduced susceptibility to neutralization circulating in Lombardy, Italy. *Viruses*  
493 **2021**.
- 494 51. Jian, F.; Yu, Y.; Song, W.; Yisimayi, A.; Yu, L.; Gao, Y.; Zhang, N.; Wang, Y.; Shao, F.; Hao, X.; et  
495 al. Further humoral immunity evasion of emerging SARS-CoV-2 BA.4 and BA.5 subvariants.  
496 **2022**, 2022.2008.2009.503384, doi:10.1101/2022.08.09.503384 %J bioRxiv.
- 497 52. Turelli, P.; Fenwick, C.; Raclot, C.; Genet, V.; Pantaleo, G.; Trono, D. P2G3 human monoclonal  
498 antibody neutralizes SARS-CoV-2 Omicron subvariants including BA.4 and BA.5 and  
499 Bebtelovimab escape mutants. **2022**, 2022.2007.2028.501852,  
500 doi:10.1101/2022.07.28.501852 %J bioRxiv.
- 501 53. Umair, M.; Ikram, A.; Salman, M.; Haider, S.A.; Badar, N.; Rehman, Z.; Ammar, M.; Rana,  
502 M.S.; Ali, Q. Genomic surveillance reveals the detection of SARS-CoV-2 delta, beta, and

- 503 gamma VOCs during the third wave in Pakistan. *Journal of medical virology* **2022**, *94*, 1115-  
504 1129, doi:10.1002/jmv.27429.
- 505 54. Ortega, J.T.; Pujol, F.H.; Jastrzebska, B.; Rangel, H.R. Mutations in the SARS-CoV-2 spike  
506 protein modulate the virus affinity to the human ACE2 receptor, an in silico analysis. *EXCLI*  
507 *journal* **2021**, *20*, 585-600, doi:10.17179/excli2021-3471.
- 508 55. Weisblum, Y.; Schmidt, F.; Zhang, F.; DaSilva, J.; Poston, D.; Lorenzi, J.C.C.; Muecksch, F.;  
509 Rutkowska, M.; Hoffmann, H.-H.; Michailidis, E.; et al. Escape from neutralizing antibodies by  
510 SARS-CoV-2 spike protein variants. *eLife* **2020**, *28*, e61312, doi:10.7554/eLife.61312.
- 511 56. Saifi, S.; Ravi, V.; Sharma, S.; Swaminathan, A.; Chauhan, N.S.; Pandey, R. SARS-CoV-2 VOCs,  
512 Mutational diversity and clinical outcome: Are they modulating drug efficacy by altered  
513 binding strength? *Genomics* **2022**, *114*, 110466, doi:10.1016/j.ygeno.2022.110466.
- 514 57. Focosi, D.; Maggi, F. Recombination in Coronaviruses, with a focus on SARS-CoV-2. *Viruses*  
515 **2022**, *14*, 1239.
- 516 58. Roemer, C.H., R; Froberg, N.; Sakaguchi, H.; Gueli, F.; Peacock, T. SARS-CoV-2 evolution,  
517 post-Omicron. Available online: [https://virological.org/t/sars-cov-2-evolution-post-](https://virological.org/t/sars-cov-2-evolution-post-omicron/911)  
518 [omicron/911](https://virological.org/t/sars-cov-2-evolution-post-omicron/911) (accessed on November 26).
- 519 59. Lambisia, A.; Nyiro, J.; Morobe, J.; Makori, T.; Ndwiga, L.; Mburu, M.; Moraa, E.; Musyoki, J.;  
520 Murunga, N.; Bejon, P.; et al. Detection of a SARS-CoV-2 Beta-like Variant with Additional  
521 Mutations in Coastal Kenya after >1 Year of Disappearance. Available online:  
522 [https://virological.org/t/detection-of-a-sars-cov-2-beta-like-variant-with-additional-](https://virological.org/t/detection-of-a-sars-cov-2-beta-like-variant-with-additional-mutations-in-coastal-kenya-after-1-year-of-disappearance/910)  
523 [mutations-in-coastal-kenya-after-1-year-of-disappearance/910](https://virological.org/t/detection-of-a-sars-cov-2-beta-like-variant-with-additional-mutations-in-coastal-kenya-after-1-year-of-disappearance/910) (accessed on November 26).
- 524 60. Sullivan, D.J.; Franchini, M.; Joyner, M.J.; Casadevall, A.; Focosi, D. Analysis of anti-Omicron  
525 neutralizing antibody titers in different convalescent plasma sources. *Nat Comm* **2022**, *13*,  
526 6478, doi:10.1038/s41467-022-33864-y.
- 527 61. Sullivan, D.J.; Franchini, M.; Senefeld, J.W.; Joyner, M.J.; Casadevall, A.; Focosi, D. Plasma  
528 after both SARS-CoV-2 boosted vaccination and COVID-19 potently neutralizes BQ1.1 and  
529 XBB. **2022**, 2022.2011.2025.517977, doi:10.1101/2022.11.25.517977 %J bioRxiv.
- 530 62. FDA Announces Bebtelovimab is Not Currently Authorized in Any US Region. Accessed online  
531 at [https://www.fda.gov/drugs/drug-safety-and-availability/fda-announces-bebtelovimab-](https://www.fda.gov/drugs/drug-safety-and-availability/fda-announces-bebtelovimab-not-currently-authorized-any-us-region)  
532 [not-currently-authorized-any-us-region](https://www.fda.gov/drugs/drug-safety-and-availability/fda-announces-bebtelovimab-not-currently-authorized-any-us-region) on December 1, 2022.
- 533 63. FDA Statement. January 24, 2022. Coronavirus (COVID-19) Update: FDA Limits Use of Certain  
534 Monoclonal Antibodies to Treat COVID-19 Due to the Omicron Variant. Accessed online at  
535 [https://www.fda.gov/news-events/press-announcements/coronavirus-covid-19-update-fda-](https://www.fda.gov/news-events/press-announcements/coronavirus-covid-19-update-fda-limits-use-certain-mono-clonal-antibodies-treat-covid-19-due-omicron)  
536 [limits-use-certain-mono-clonal-antibodies-treat-covid-19-due-omicron](https://www.fda.gov/news-events/press-announcements/coronavirus-covid-19-update-fda-limits-use-certain-mono-clonal-antibodies-treat-covid-19-due-omicron) on February 3, .
- 537 64. FDA updates Sotrovimab emergency use authorization. March 30, 2022. Accessed online at  
538 [https://www.fda.gov/drugs/drug-safety-and-availability/fda-updates-sotrovimab-](https://www.fda.gov/drugs/drug-safety-and-availability/fda-updates-sotrovimab-emergency-use-authorization)  
539 [emergency-use-authorization](https://www.fda.gov/drugs/drug-safety-and-availability/fda-updates-sotrovimab-emergency-use-authorization) on April 26, 2022.
- 540 65. FDA releases important information about risk of COVID-19 due to certain variants not  
541 neutralized by Evusheld. Accessed online at [https://www.fda.gov/drugs/drug-safety-and-](https://www.fda.gov/drugs/drug-safety-and-availability/fda-releases-important-information-about-risk-covid-19-due-certain-variants-not-neutralized-evusheld#:~:text=Therefore%2C%20on%20June%2029%2C%202022,if%20patients%20need%20ongoing%20protection)  
542 [availability/fda-releases-important-information-about-risk-covid-19-due-certain-variants-](https://www.fda.gov/drugs/drug-safety-and-availability/fda-releases-important-information-about-risk-covid-19-due-certain-variants-not-neutralized-evusheld#:~:text=Therefore%2C%20on%20June%2029%2C%202022,if%20patients%20need%20ongoing%20protection)  
543 [not-neutralized-](https://www.fda.gov/drugs/drug-safety-and-availability/fda-releases-important-information-about-risk-covid-19-due-certain-variants-not-neutralized-evusheld#:~:text=Therefore%2C%20on%20June%2029%2C%202022,if%20patients%20need%20ongoing%20protection)  
544 [evusheld#:~:text=Therefore%2C%20on%20June%2029%2C%202022,if%20patients%20need](https://www.fda.gov/drugs/drug-safety-and-availability/fda-releases-important-information-about-risk-covid-19-due-certain-variants-not-neutralized-evusheld#:~:text=Therefore%2C%20on%20June%2029%2C%202022,if%20patients%20need%20ongoing%20protection)  
545 [%20ongoing%20protection](https://www.fda.gov/drugs/drug-safety-and-availability/fda-releases-important-information-about-risk-covid-19-due-certain-variants-not-neutralized-evusheld#:~:text=Therefore%2C%20on%20June%2029%2C%202022,if%20patients%20need%20ongoing%20protection). on October 10, 2022.
- 546 66. Senefeld, J.W.; Klassen, S.A.; Ford, S.K.; Senese, K.A.; Wiggins, C.C.; Bostrom, B.C.;  
547 Thompson, M.A.; Baker, S.E.; Nicholson, W.T.; Johnson, P.W.; et al. Use of convalescent  
548 plasma in COVID-19 patients with immunosuppression. *Transfusion* **2021**, *61*, 2503-2511,  
549 doi:10.1111/trf.16525.
- 550 67. Chen, C.; Nadeau, S.; Yared, M.; Voinov, P.; Xie, N.; Roemer, C.; Stadler, T. CoV-Spectrum:  
551 analysis of globally shared SARS-CoV-2 data to identify and characterize new variants.  
552 *Bioinformatics* **2021**, *38*, 1735-1737, doi:10.1093/bioinformatics/btab856 %J Bioinformatics.

553 68. Hadfield, J.; Megill, C.; Bell, S.M.; Huddleston, J.; Potter, B.; Callender, C.; Sagulenko, P.;  
554 Bedford, T.; Neher, R.A. Nextstrain: real-time tracking of pathogen evolution. *Bioinformatics*  
555 **2018**, *34*, 4121-4123, doi:10.1093/bioinformatics/bty407 %J Bioinformatics.

556

557 **Table 1**

558 Heatmap of selected Spike RBD mutations in Omicron sublineages and their impact on authorized therapeutic anti-Spike mAbs. BAM: bamlanivimab; ETE:  
 559 etesevimab; CAS: casirivimab; IMD: imdevimab; TIX: tixagevimab; CIL: cilgavimab; SOT: sotrovimab; BEB: bebtelovimab; REG: regdanvimab. Data sourced  
 560 from the Stanford University Coronavirus and Antiviral Resistance Database (accessed online at <https://covdb.stanford.edu/search-drdb>  
 561 2022). Green means fold-reductions < 5; Orange means fold-reduction 5-100 ; Red means fold-reduction in IC<sub>50</sub> > 100 compared to wild-type; blank means  
 562 no data available.

Spike mutation		Main lineages	BAM	ETE	CAS	IMD	CIL	TIX	SOT	BEB	REG
R346X	T	BS.1.*, BP.1, DD.1, BJ.1, BL.1.*, BL.2.*, BL.5, BA.2.75.2.* (CA.*), BM.1.1.* (CJ.* and CV.*), BM.4.1.1.1.* (CH.*), BR.2.* and BR.3, BN.1, BA.2.75.6.* (BY.*), BA.2.75.9.* (CY.*), BA.2.76, BA.4.1.8 and BA.4.1.9, CS.1, BA.4.6.* (DC.*) and BA.4.7, BA.5.1.18 and BA.5.1.20, DE.2, BA.5.1.26.* (CU.*), BA.5.1.27 and BA.5.1.28, BF.7.*, BF.11.*, BA.5.2.6.* (CP.*), BA.5.2.13.* (CR.*), BA.5.2.25.* (DA.*), BA.5.2.39, BQ.1.1.* (CZ.*, CW.*, DK.*), BE.1.2.*, BE.1.4.2, BE.4.1.* (CQ.*), BE.5, BE.6 and BE.7, XBB.*, XBD, XBE, XBF, XBG									
	E	BA.5.6.4									
	I	BF.33, CE.1									
	R	BA.5.2.25, DB.2									
	S	BL.5, BF.13, BQ.1.21, BE.6									
K444X	M	CA.3.1, BR.1.*, BA.5.2.7, CY.1, BU.1, CG.1, BQ.1.17									
	N	BA.2.38.*, BA.4.6.3, BA.5.1.29, BV.2, BA.5.2.24, CK.* (DG.*), BE.4.2									
	R	BA.2.3.20.* (CM.*), CS.1, BF.16, BA.5.2.18, CR.1.*, CR.2, BA.5.2.41, CQ.1.*, XBB.4.*									
	T	CH.1.*, BR.4, BA.5.2.25, DB.1, DB.2, BA.5.2.36.* (CT.1), BE.1.1.1, BQ.1.* (CZ.*, CW.*, DK.*), BQ.2, BE.9,									





	P	BA.2.10.4, CA.4, CJ.1, XBB.1.5, XBC.* , XBF										
	S	BA.2.75.2.* (CA.*), BM.1.* (CV.*), BM.4.1.* (CH.*), BR.1.2, BY.1.* , BA.2.75.7, XBB.* , XBD										
	V	BM.2.1, CB.1, BA.4.* (CS.* , DC.*), BA.5.* (BT.* , DH.* , DE.* , CU.* , CL.* , BF.* , BZ.* , CP.* , CY.* , BU.* , CR.* , BV.* , CN.* , CK.* , DG.* , DB.* , CG.* , CF.* , CD.* , CE.* , CT.* , DA.* , BE.* , BQ.* , CZ.* , CW.* , CC.* , CQ.* , BW.* , DK.*), XBE, XBG										
F490X	I	CZ.1										
	L	BL.1.3										
	S	BM.1.1.1.* (CJ.1), BN.1.* , BN.2.1., BN.3.1, BN.4, XBB.* , XBF										
	V	BJ.1, BL.1.4										
R493X	L	BA.2.3.21.1										
	Q	BA.2.10.4, BA.2.75.* (BL.* , CA.* , BM.* , CJ.* , CV.* , CH.* , BR.* , BN.* , BY.* , CB.*), BA.4.* (CS.* , DC.*), BA.5.* (BT.* , DH.* , DE.* , CU.* , CL.* , BF.* , BZ.* , CP.* , CY.* , BU.* , CR.* , BV.* , CN.* , CK.* , DG.* , DB.* , CG.* , CF.* , CD.* , CE.* , CT.* , DA.* , BE.* , BQ.* , CZ.* , CW.* , CC.* , CQ.* , BW.* , DK.*), XBB.* , XBC.* , XBD, XBE, XBF, XBG										
S494P		BA.2.10.4, CA.2, BN.1.* ,BY.1.2.1, BQ.1.1.11, BQ.1.1.12, BQ.1.19										

564 **Supplementary Table 1**

565 Occurrence of selected amino acid mutations associated with immune escape within the Spike protein of SARS-CoV-2 in BA.2 and BA.4/5 Omicron  
 566 sublineages. Modified from [https://docs.google.com/spreadsheets/d/1OTWogpyvWNTIK0ww7TIDcl4l\\_SkZt3Z8nYiSp2YARys/edit?usp=sharing](https://docs.google.com/spreadsheets/d/1OTWogpyvWNTIK0ww7TIDcl4l_SkZt3Z8nYiSp2YARys/edit?usp=sharing)

<b>PANGO lineage</b>	<b>nickname</b>	<b>Y 144del</b>	<b>R 346</b>	<b>K 356</b>	<b>K 444</b>	<b>V 445</b>	<b>G 446</b>	<b>N 450</b>	<b>L 452</b>	<b>N 460</b>	<b>F 486</b>	<b>F 490</b>	<b>R 493</b>	<b>S 494</b>
<b>BA.1</b>							S							
<b>BA.1.1</b>			K				S							
<b>BA.2</b>														
<b>BA.2.3</b>														
<b>BA.2.3.2</b>														
<b>BS.1</b>			T						R	K			Q	
BS.1.1			T	T					R	K			Q	
BS.1.2			T						R	K			Q	
<b>BA.2.3.16</b>														
BP.1			T						M					
<b>BA.2.3.20</b>	Basilisk				R			D	M	K			Q	
CM.1					R			D	M	K			Q	
CM.2					R			D	M	K			Q	
CM.3					R			D	M	K			Q	
CM.4					R			D	M	K			Q	
<b>CM.5</b>					R			D	M	K			Q	
CM.5.1					R			D	M	K			Q	
<b>CM.6</b>					R			D	M	K			Q	
CM.6.1					R			D	M	K			Q	
CM.7					R			D	M	K	S		Q	
<b>CM.8</b>					R		S	D	M	K			Q	
CM.8.1					R		S	D	M	K	S		Q	

CM.9					R			D	M	K			Q	
<b>BA.2.3.21</b>													Q	
DD.1			T							K			L	
<b>BA.2.10</b>														
<b>BA.2.10.1</b>														
BJ.1	Argus		T			P	S					V		
BA.2.10.4							S				P		Q	P
<b>BA.2.38</b>														
BA.2.38.1					N									
BA.2.38.2					N									
<b>BA.2.38.3</b>														
BH.1							S		Q					
BA.2.38.4					N									
<b>BA.2.75</b>	Centaurus						S			K			Q	
<b>BA.2.75.1</b>							S			K			Q	
<b>BL.1</b>			T				S			K			Q	
BL.1.1			T				S			K			Q	
BL.1.2			T				S			K			Q	
BL.1.3			T				S			K		L	Q	
BL.1.4			T				S			K		V	Q	
<b>BL.2</b>			T				S			K			Q	
BL.2.1			T				S			K			Q	
BL.3							S			K			Q	
BL.4							S			K			Q	
BL.5			S				S			K			Q	
<b>BA.2.75.2</b>	Chiron		T				S			K	S		Q	
CA.1			T				S		R	K	S		Q	
CA.2			T				S			K	S		Q	P

<b>CA.3</b>			T			S			K	S		Q
CA.3.1			T	M		S		R	K	S		Q
CA.4			T			S			K	P		Q
CA.5			T			S			K	S		Q
CA.6			T			S			K	S		Q
CA.7			T			S		R	K	S		Q
<b>BA.2.75.3</b>						S			K			Q
<b>BM.1</b>						S			K	S		Q
<b>BM.1.1</b>			T			S			K	S		Q
<b>BM.1.1.1</b>	Mimas		T			S			K	S	S	Q
CJ.1			T			S			K	P	S	Q
BM.1.1.2			T			S			K	S		Q
<b>BM.1.1.3</b>			T			S			K	S		Q
CV.1			T			S		R	K	S		Q
<b>BM.2</b>			T			S			K			Q
BM.2.1			T			S			K	V		Q
BM.2.2			T			S			K			Q
BM.2.3			T			S			K	I		Q
BM.3						S			K			Q
<b>BM.4</b>						S			K			Q
<b>BM.4.1</b>						S			K	S		Q
<b>BM.4.1.1</b>			T			S			K	S		Q
<b>CH.1</b>			T	T		S			K	S		Q
CH.1.1			T	T		S		R	K	S		Q
CH.2			T			S			K	S		Q
BM.5						S			K			Q
BM.6						S			K			Q
<b>BA.2.75.4</b>						S		R	K			Q

<b>BR.1</b>					M		S		R	K			Q	
BR.1.1					M		S		R	K			Q	
BR.1.2					M		S		R	K	S		Q	
<b>BR.2</b>			T				S		R	K	I		Q	
BR.2.1			T				S		R	K	I		Q	
BR.3			T				S		R	K			Q	
BR.4					T		G		R	K			Q	
<b>BA.2.75.5</b>				T			S			K			Q	
<b>BN.1</b>	Hydra		T	T			S			K		S	Q	
<b>BN.1.1</b>			T	T			S			K		S	Q	P
BN.1.1.1			T	T			S			K		S	Q	P
<b>BN.1.2</b>			T	T			S			K		S	Q	
BN.1.2.1			T	T			S			K		S	Q	
<b>BN.1.3</b>			T	T			S			K		S	Q	
BN.1.3.1			T	T			S			K		S	Q	
BN.1.4			T	T			S			K		S	Q	
BN.1.5			T	T			S			K		S	Q	
BN.1.6			T	T			S			K		S	Q	
BN.1.7			T	T			S			K		S	Q	
<b>BN.2</b>				T			S			K			Q	
BN.2.1				T			S			K		S	Q	
<b>BN.3</b>				T			S	D		K			Q	
BN.3.1				T			S	D		K		S	Q	
BN.4				T			S			K		S	Q	
BN.5				T			S			K			Q	
BN.6				T			S			K			Q	
<b>BA.2.75.6</b>	Dictys		T				S			K			Q	
<b>BY.1</b>			T				S			K	S		Q	

<b>BY.1.1</b>			T				S		R	K	S		Q	
BY.1.1.1			T				S		R	K	S		Q	
<b>BY.1.2</b>			T				S			K	S		Q	P
BY.1.2.1			T				S			K	S		Q	
BA.2.75.7							S			K	S		Q	
BA.2.75.8							S		Q	K			Q	
<b>BA.2.75.9</b>			T				S			K			Q	
CB.1			T				S			K	V		Q	
BA.2.75.10							S			K			Q	
BA.2.76			T											
<b>BA.4</b>									R		V		Q	
<b>BA.4.1</b>									R		V		Q	
BA.4.1.8			T						R		V		Q	
BA.4.1.9	Cetus		T						R		V		Q	
<b>BA.4.1.10</b>			T						R		V		Q	
CS.1			T		R				R		V		Q	
<b>BA.4.6</b>	Aeterna		T						R		V		Q	
BA.4.6.1			T						R		V		Q	
BA.4.6.2			T			A			R		V		Q	
BA.4.6.3			T		N				R	K	V		Q	
BA.4.6.4			T						R		V		Q	
<b>BA.4.6.5</b>			T						R		V		Q	
DC.1			T						R	S	V		Q	
BA.4.7			T						R		V		Q	
BA.4.8									R		V		Q	
<b>BA.5</b>									R		V		Q	
<b>BA.5.1</b>	Sphinx								R		V		Q	
BA.5.1.18			T						R		V		Q	

BA.5.1.19								R		V		Q
BA.5.1.20			T					R		V		Q
<b>BA.5.1.21</b>								R		V		Q
BT.1								R		V		Q
BT.2								R		V		Q
<b>BA.5.1.22</b>								R		V		Q
DH.1								R		V		Q
<b>BA.5.1.23</b>								R		V		Q
DE.1								R		V		Q
DE.2			T					R		V		Q
BA.5.1.24								R		V		Q
BA.5.1.25								R		V		Q
<b>BA.5.1.26</b>			T					R		V		Q
CU.1			T					R		V		Q
BA.5.1.27			T					R		V		Q
BA.5.1.28			T					R		V		Q
<b>BA.5.1.29</b>					N			R		V		Q
CL.1								R	K	V		Q
BA.5.1.30								R		V		Q
<b>BA.5.2</b>	Triton							R		V		Q
<b>BA.5.2.1</b>								R		V		Q
<b>BF.1</b>								R		V		Q
BF.1.1								R		V		Q
BF.2								R		V		Q
<b>BF.3</b>								R		V		Q
BF.3.1							S	R		V		Q
BF.4								R		V		Q
BF.5								R		V		Q

BF.6									R		V		Q
<b>BF.7</b>	Minotaur		T						R		V		Q
BF.7.1			T						R		V		Q
BF.7.2			T						R		I		Q
BF.7.3			T						R		V		Q
<b>BF.7.4</b>			T						R		V		Q
BF.7.4.1			T						R		V		Q
BF.7.4.2			T						R		V		Q
<b>BF.7.5</b>			T						R		V		Q
BF.7.5.1			T						R		V		Q
BF.7.6			T						R		V		Q
BF.7.7			T						R		V		Q
BF.7.8			T						R		V		Q
BF.7.9			T						R		V		Q
BF.7.10			T						R		V		Q
BF.7.11			T						R		V		Q
BF.7.12			T						R		V		Q
<b>BF.7.13</b>			T						R		V		Q
BF.7.13.1			T						R		V		Q
BF.7.13.2			T						R		V		Q
BF.8									R		V		Q
BF.9									R		V		Q
BF.10									R		V		Q
<b>BF.11</b>	Python		T						R		V		Q
BF.11.1			T						R		V		Q
BF.11.2			T						R		V		Q
BF.11.3			T						R		V		Q
BF.11.4			T						R		V		Q



BF.11.5			T					R		V		Q
BF.12								R		I		Q
BF.13			S					R		V		Q
BF.14							D	R		V		Q
BF.15								R		V		Q
BF.16					R			R		V		Q
BF.17								R		V		Q
BF.18								R		V		Q
BF.19								R		V		Q
BF.20								R		V		Q
BF.21								R		V		Q
BF.22								R		V		Q
BF.23								R		V		Q
BF.24								R		V		Q
BF.25					A			R		V		Q
BF.26								R		V		Q
BF.27								R		V		Q
BF.28								R		V		Q
BF.29								R		V		Q
BF.30			T					R		V		Q
<b>BF.31</b>								R		V		Q
BF.31.1								R		V		Q
BF.32							D	R		V		Q
BF.33			I					R	K	V		Q
BF.34			T					R		V		Q
<b>BA.5.2.3</b>								R		V		Q
BZ.1								R		V		Q
<b>BA.5.2.6</b>			T					R		V		Q

<b>CP.1</b>			T					R		V		Q
CP.1.1			T		A			R		V		Q
CP.1.2			T					R		V		Q
CP.1.3			T			S		R		V		Q
CP.2			T					R		V		Q
CP.3			T					R	Y	V		Q
CP.4			T					R		V		Q
CP.5			T					R		V		Q
CP.6			T					R		V		Q
<b>BA.5.2.7</b>					M			R		V		Q
CY.1					M			R	K	V		Q
BA.5.2.13			T					R		V		Q
<b>BA.5.2.16</b>								R		V		Q
BU.1					M			R	K	V		Q
BU.2						A		R		V		Q
BU.3							D	R		V		Q
<b>BA.5.2.18</b>					R			R		V		Q
<b>CR.1</b>			T		R			R		V		Q
CR.1.1			T		R			R		V		Q
CR.1.2			T		R	A		R		V		Q
CR.2					R			R		V		Q
BA.5.2.19								R		V		Q
<b>BA.5.2.20</b>								R		V		Q
BV.1								R		V		Q
BV.2					N			R		V		Q
<b>BA.5.2.21</b>								R		V		Q
CN.1							D	R		V		Q
BA.5.2.22								R		V		Q

BA.5.2.23						A			R		V		Q
<b>BA.5.2.24</b>				N					R		V		Q
CK.1				N					R	K	V		Q
<b>CK.2</b>				N					R		V		Q
<b>CK.2.1</b>				N					R	K	V		Q
<b>CK.2.1.1</b>				N					R	K	V		Q
DG.1				N					R	K	V		Q
CK.3				N					R	K	V		Q
<b>BA.5.2.25</b>			R	T					R		V		Q
DB.1			T	T					R	K	V		Q
DB.2			R	T					R		V		Q
<b>BA.5.2.26</b>									R		V		Q
CG.1				M					R		V		Q
<b>BA.5.2.27</b>									R		V		Q
CF.1									R		V		Q
BA.5.2.28									R		V		Q
BA.5.2.29									R		V		Q
BA.5.2.30							D		R		V		Q
<b>BA.5.2.31</b>									R		V		Q
CD.1							D		R		V		Q
CD.2									R		V		Q
BA.5.2.32								D	R		V		Q
<b>BA.5.2.33</b>									R		V		Q
CE.1			I						R		V		Q
BA.5.2.34			T						R		V		Q
BA.5.2.35			T						R		V		Q
<b>BA.5.2.36</b>				T					R		V		Q
CT.1				T	T				R		V		Q

BA.5.2.37								R		V		Q	
<b>BA.5.2.38</b>								R		V		Q	
DA.1			T					R		V		Q	
BA.5.2.39			T					R		V		Q	
BA.5.2.40							D	R		V		Q	
BA.5.2.41					R			R		V		Q	
<b>BA.5.3</b>								R		V		Q	
<b>BA.5.3.1</b>								R		V		Q	
<b>BE.1</b>								R		V		Q	
<b>BE.1.1</b>								R		V		Q	
<b>BE.1.1.1</b>					T			R		V		Q	
<b>BQ.1</b>	Typhon				T			R	K	V		Q	
<b>BQ.1.1</b>	Cerberus		T		T			R	K	V		Q	
<b>BQ.1.1.1</b>			T		T			R	K	V		Q	
CZ.1			T		T			R	K	V	I	Q	
BQ.1.1.2			T		T			R	K	V		Q	
BQ.1.1.3			T		T			R	K	V		Q	
BQ.1.1.4			T		T			R	K	V		Q	
BQ.1.1.5			T		T			R	K	V		Q	
BQ.1.1.6			T		T			R	K	V		Q	
BQ.1.1.7			T		T			R	K	V		Q	
BQ.1.1.8			T		T			R	K	V		Q	
BQ.1.1.9			T		T			R	K	V		Q	
BQ.1.1.10			T		T			R	K	V		Q	
BQ.1.1.11			T		T			R	K	V		Q	P
BQ.1.1.12			T		T			R	K	V		Q	P
BQ.1.1.13			T		T			R	K	V		Q	
<b>BQ.1.1.14</b>			T		T			R	K	V		Q	

CW.1			T		T		S		R	K	V		Q
BQ.1.1.15			T		T				R	K	V		Q
BQ.1.1.16			T		T				R	K	V		Q
BQ.1.1.17			T		T				R	K	V		Q
BQ.1.1.18			T		T				R	K	V		Q
BQ.1.1.19			T		T				R	K	V		Q
BQ.1.1.20			T		T				R	K	V		Q
BQ.1.1.21			T		T				R	K	V		Q
BQ.1.1.22			T		T				R	K	V		Q
BQ.1.1.23			T		T				R	K	V		Q
BQ.1.1.24			T		T				R	K	V		Q
BQ.1.2					T				R	K	V		Q
BQ.1.3					T				R	K	V		Q
BQ.1.4					T				R	K	V		Q
BQ.1.5					T				R	K	V		Q
BQ.1.6					T				R	K	V		Q
BQ.1.7					T				R	K	V		Q
<b>BQ.1.8</b>					T				R	K	V		Q
BQ.1.8.1					T				R	K	V		Q
BQ.1.8.2					T				R	K	V		Q
BQ.1.9			T		T				R	K	V		Q
<b>BQ.1.10</b>					T				R	K	V		Q
BQ.1.10.1					T				R	K	V		Q
BQ.1.11					T				R	K	V		Q
BQ.1.12					T				R	K	V		Q
BQ.1.13					T				R	K	V		Q
BQ.1.14					T				R	K	V		Q
BQ.1.15					T				R	K	V		Q

BQ.1.16				T				R	K	V		Q	
BQ.1.17				M				R	K	V		Q	
BQ.1.18			T	T				R	K	V		Q	P
BQ.1.19				T				R	K	V		Q	
BQ.1.20				T				R	K	V		Q	
BQ.1.21			S	T				R	K	V		Q	
BQ.1.22			T	T				R	K	V		Q	
BQ.1.23				T				R	K	V		Q	
BQ.1.24			T	T				R	K	V		Q	
BQ.1.25			T	T				R	K	V		Q	
BQ.1.26				T				R	K	V		Q	
BQ.2				T				R		V		Q	
<b>BE.1.1.2</b>								R		V		Q	
CC.1							D	R		V		Q	
<b>BE.1.2</b>			T					R		V		Q	
BE.1.2.1			T		A			R		V		Q	
BE.1.3								R		V		Q	
<b>BE.1.4</b>								R		V		Q	
BE.1.4.1								R		V		Q	
BE.1.4.2			T					R		V		Q	
BE.1.4.3					A			R		V		Q	
BE.1.4.4								R		V		Q	
BE.2								R		V		Q	
BE.3								R		V		Q	
<b>BE.4</b>								R		V		Q	
<b>BE.4.1</b>			T					R		V		Q	
<b>BE.4.1.1</b>			T		R			R		V		Q	
<b>CQ.1</b>			T		R			R		V		Q	

CQ.1.1			T		R				R		V		Q
CQ.2			T		R	A			R		V		Q
BE.4.2					N				R	K	V		Q
BE.5			T						R		V		Q
BE.6			S						R		V		Q
BE.7			T						R		V		Q
BE.8			T						R		V		Q
BE.9					T				R	K	V		Q
BA.5.3.5			T						R		V		Q
<b>BA.5.5</b>									R		V		Q
BA.5.5.3									R		V		Q
<b>BA.5.6</b>									R		V		Q
<b>BA.5.6.2</b>					T				R		V		Q
BW.1					T				R	K	V		Q
BA.5.6.3			T						R		V		Q
BA.5.6.4			E						R		V		Q
<b>BA.5.10</b>									R		V		Q
<b>BA.5.10.1</b>			T						R		V		Q
DF.1			T						R		V		Q
BA.5.11			T						R		V		Q
<b>XBB</b>	Gryphon		T			P	S			K	S	S	Q
<b>XBB.1</b>			T			P	S			K	S	S	Q
XBB.1.1			T			P	S			K	S	S	Q
XBB.1.2			T			P	S			K	S	S	Q
XBB.1.3			T			P	S			K	S	S	Q
XBB.1.4			T			P	S			K	S	S	Q
XBB.1.5			T			P	S			K	P	S	Q
XBB.2			T			P	S			K	S	S	Q

<b>XBB.3</b>			T			P	S			K	S	S	Q	
XBB.3.1			T			P	S			K	S	S	Q	
<b>XBB.4</b>			T		R	P	S			K	S	S	Q	
XBB.4.1			T		R	P	S			K	S	S	Q	
XBB.5			T			P	S			K	S	S	Q	
<b>XBC</b>							S				P		Q	
XBC.1							S		M		P		Q	
XBC.2							S				P		Q	
XBD			T				S		L	K	S		Q	
XBE			T						R		V		Q	
XBF			T				S			K	P	S	Q	
XBG			T						R		V		Q	

567

568

569



570

## Figure 1

571

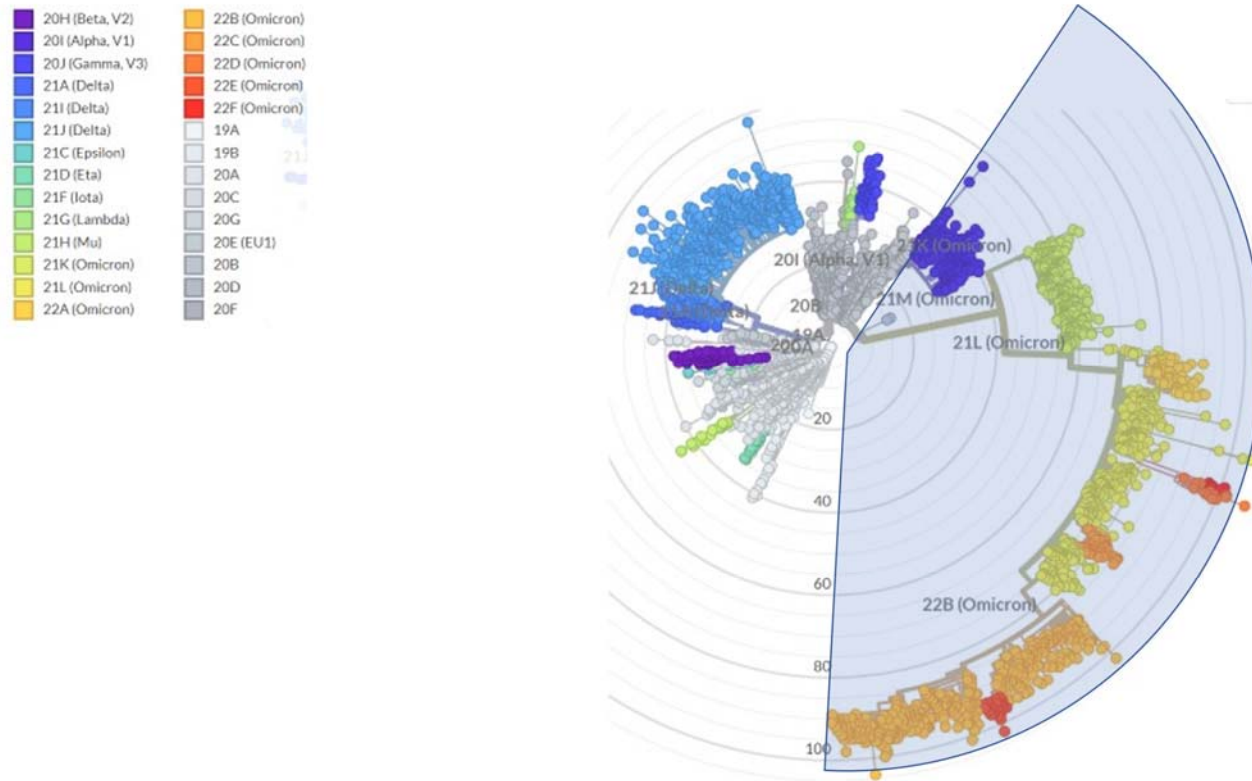
Radial tree of SARS-CoV-2 evolution, with branch length approximating divergence, showing that Omicron (light blue shadow) currently includes more than

572

45% or variations across 3045 genomes sampled between Dec 2019 and Nov 2022. Accessed online at [https://nextstrain.org/ncov/gisaid/global/all-](https://nextstrain.org/ncov/gisaid/global/all-time?l=radial&m=div)

573

[time?l=radial&m=div](https://nextstrain.org/ncov/gisaid/global/all-time?l=radial&m=div) on November 26, 2022.



574

575

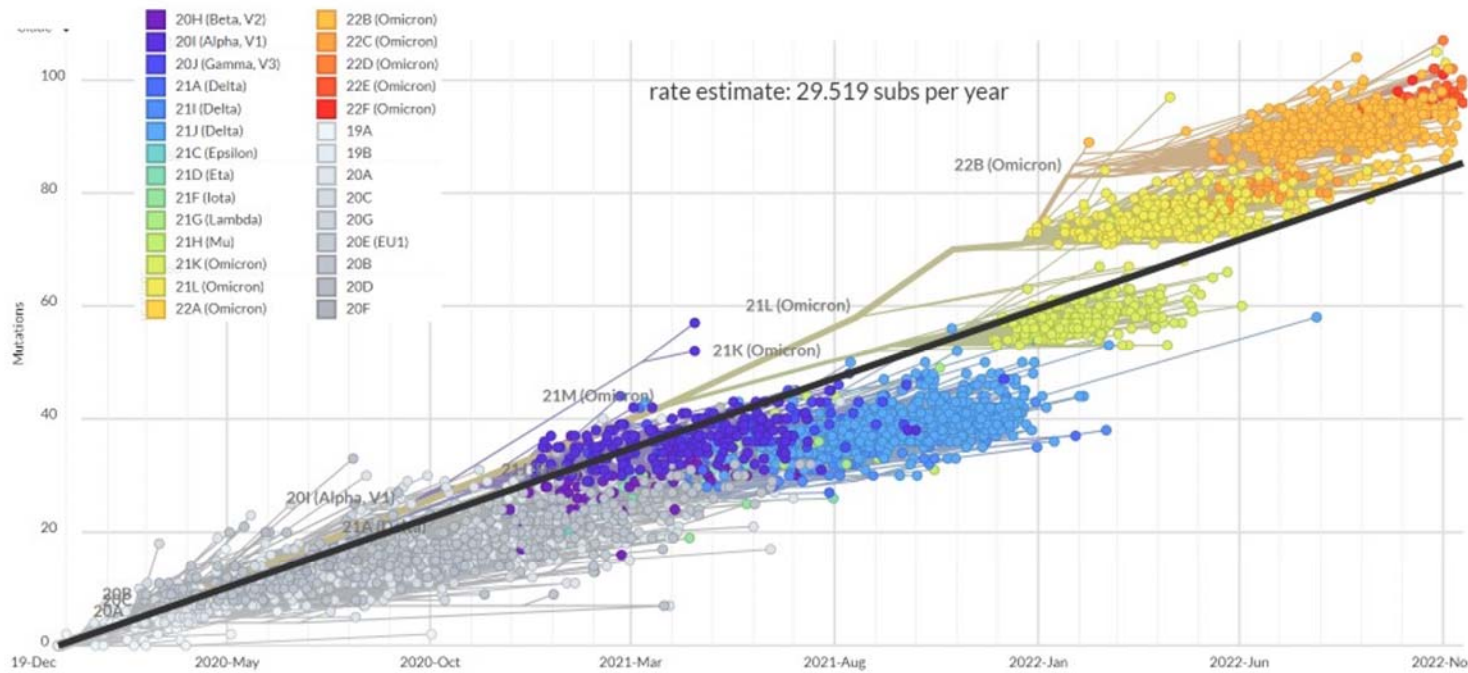
## Figure 2

576

Clock tree of SARS-CoV-2 evolution, with regression line showing an increase in the estimate rate of substitutions per year across 3045 genomes sampled

577

between Dec 2019 and Nov 2022. Accessed online at <https://nextstrain.org/ncov/gisaid/global/all-time?l=clock&m=div> on November 26, 2022.



578

579

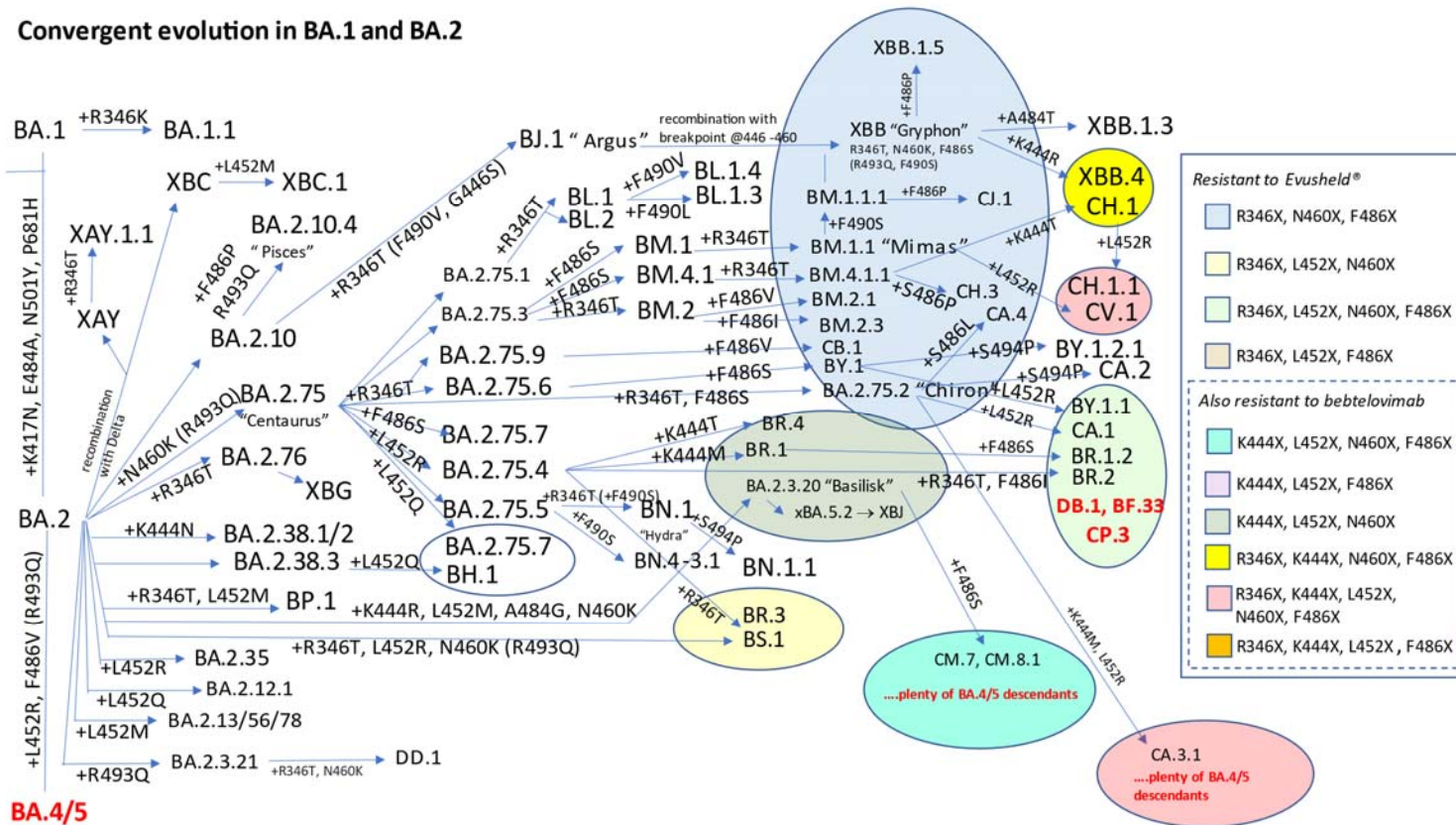
### Figure 3

580

Diagram representing all SARS-CoV-2 Omicron sublineages designated by PANGOLIN as of November 26, 2022 for which at least one of the Spike RBD immune escaping mutations (R346X, K444X, L452X, N460X, F486X, or R493Q) represents a branching event. Mythological names introduced by Ryan T Gregory and used colloquially are also reported. Convergence towards combos of this mutations is noted, with different background colors representing different combinations. Resistance of each combination to clinically authorized anti-Spike mAbs is reported on the right box. For visualization purposes, the upper panel shows BA.1 and BA.2 evolution, while the lower panel shows BA.4/5 evolution.

584

#### Convergent evolution in BA.1 and BA.2



585



587

## Figure 4

588

**Step-wise accumulation of key Spike mutations involved in immune escape within SARS-CoV-2 Omicron sublineages increase the relative growth rate.**

589

Lineage name text is color coded, where BA.5 descendants are in blue text, BA.4 descendants in green text and BA.2.75 descendants are in red text. Each

590

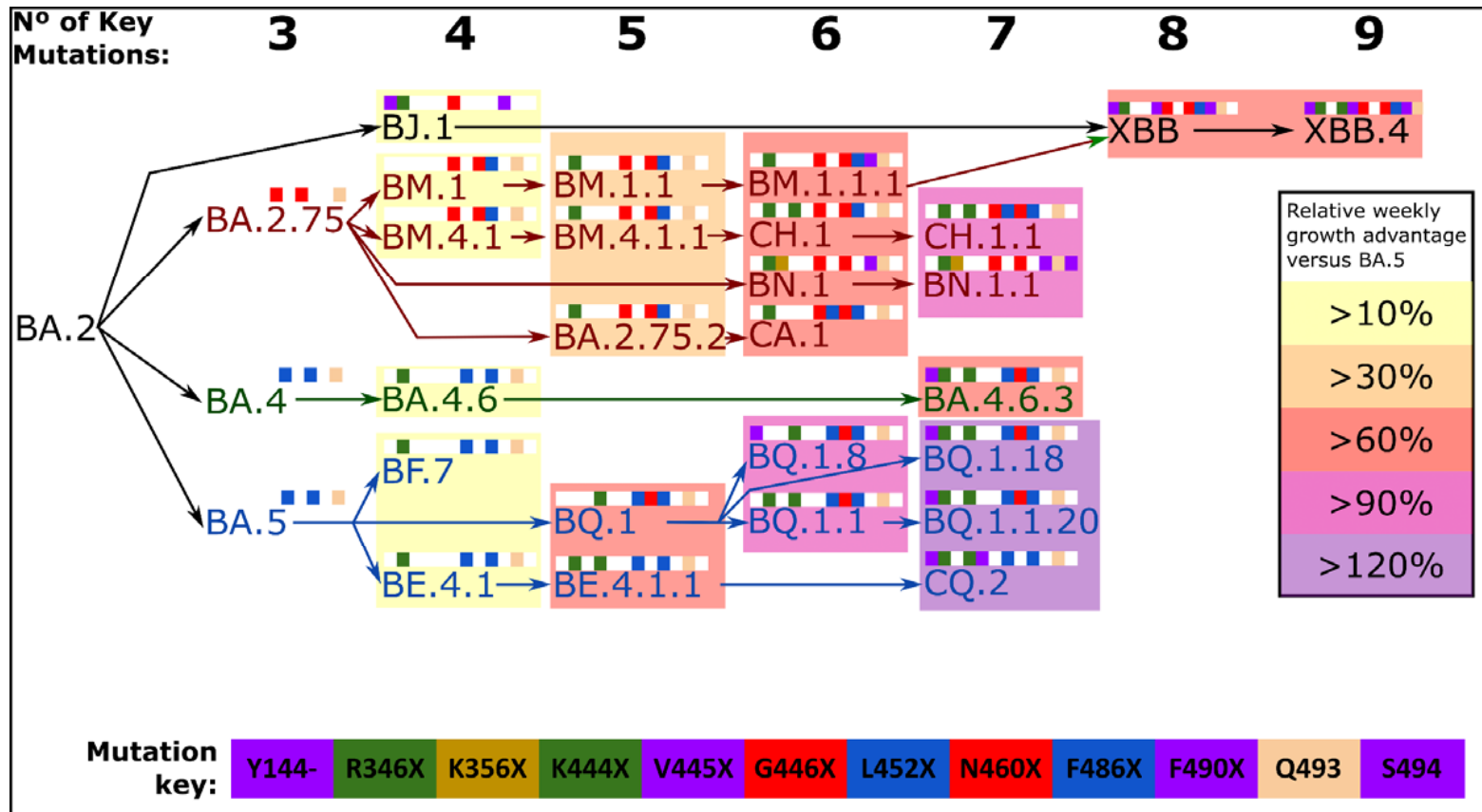
mutation is color coded as shown in the mutation key, and depicted as colored squares when present or white squares if absent. Number of key mutations

591

of each lineage is summarized at the top. Relative growth rates were calculated using BA.5 lineage as baseline, for groups of BA.4, BA.5, BA.2.75 and XBB

592

descendant lineages with each exact total number of key mutations. Relative growth rates were calculated using CoV-Spectrum [67]



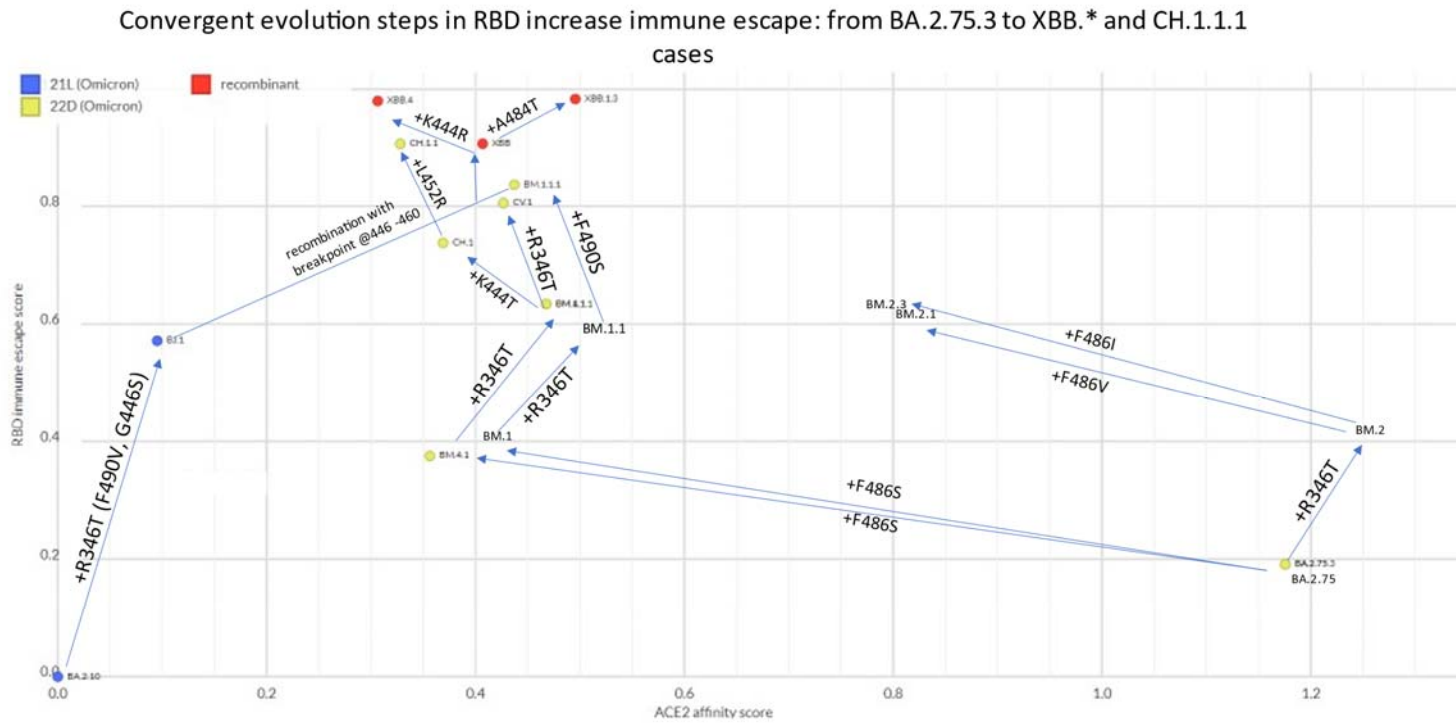
593

594

595  
596  
597  
598  
599

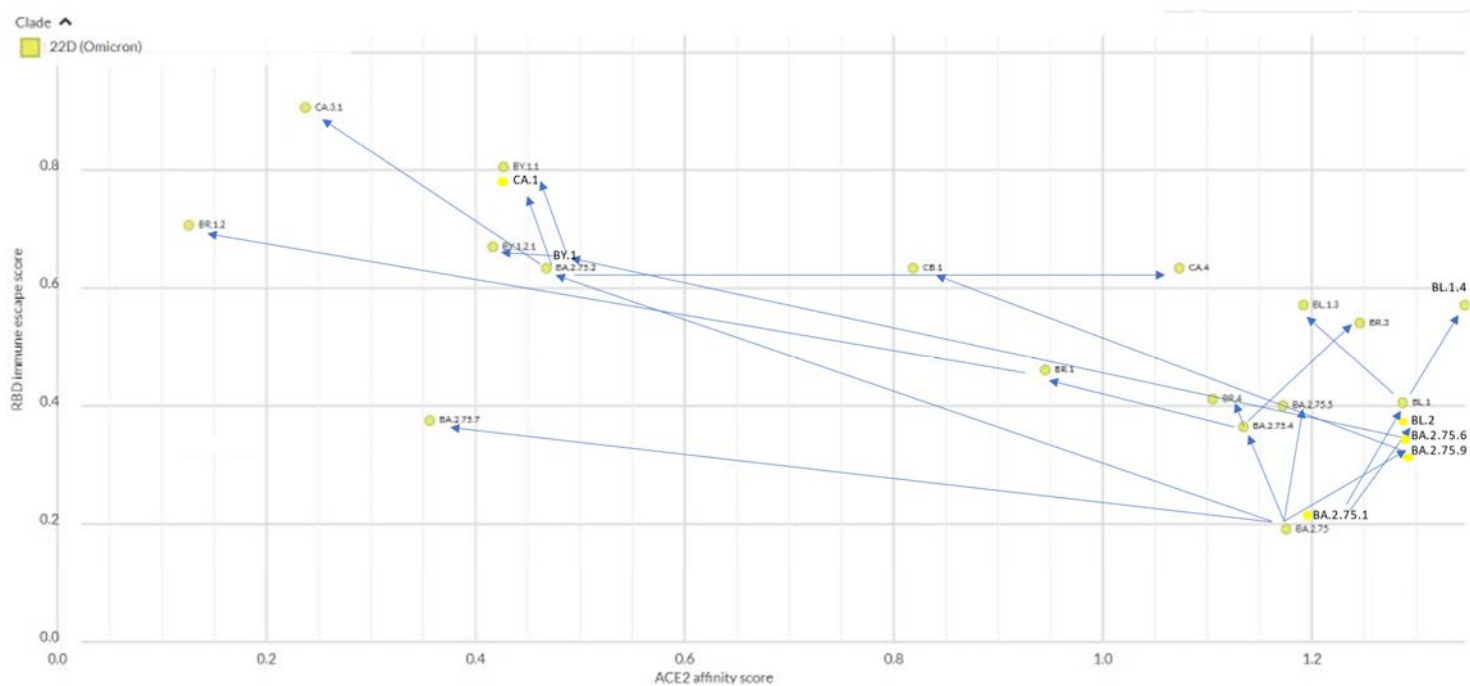
## Figure 5

**Evolutionary steps at the basis of the major Omicron branches (CZ.1, XBB.\* and CH.1.1.1, and other BA.2.75.\* descendants), showing progressive increases in RBD immune escape score (as calculated here: [https://jbloomlab.github.io/SARS2\\_RBD\\_Ab\\_escape\\_maps/escape-calc/](https://jbloomlab.github.io/SARS2_RBD_Ab_escape_maps/escape-calc/)). Chart created on NextStrain [68] ([https://next.nextstrain.org/staging/nextclade/sars-cov-2/21L?gmin=15&l=scatter&scatterX=ace2\\_binding&scatterY=immune\\_escape&showBranchLabels=all](https://next.nextstrain.org/staging/nextclade/sars-cov-2/21L?gmin=15&l=scatter&scatterX=ace2_binding&scatterY=immune_escape&showBranchLabels=all))**



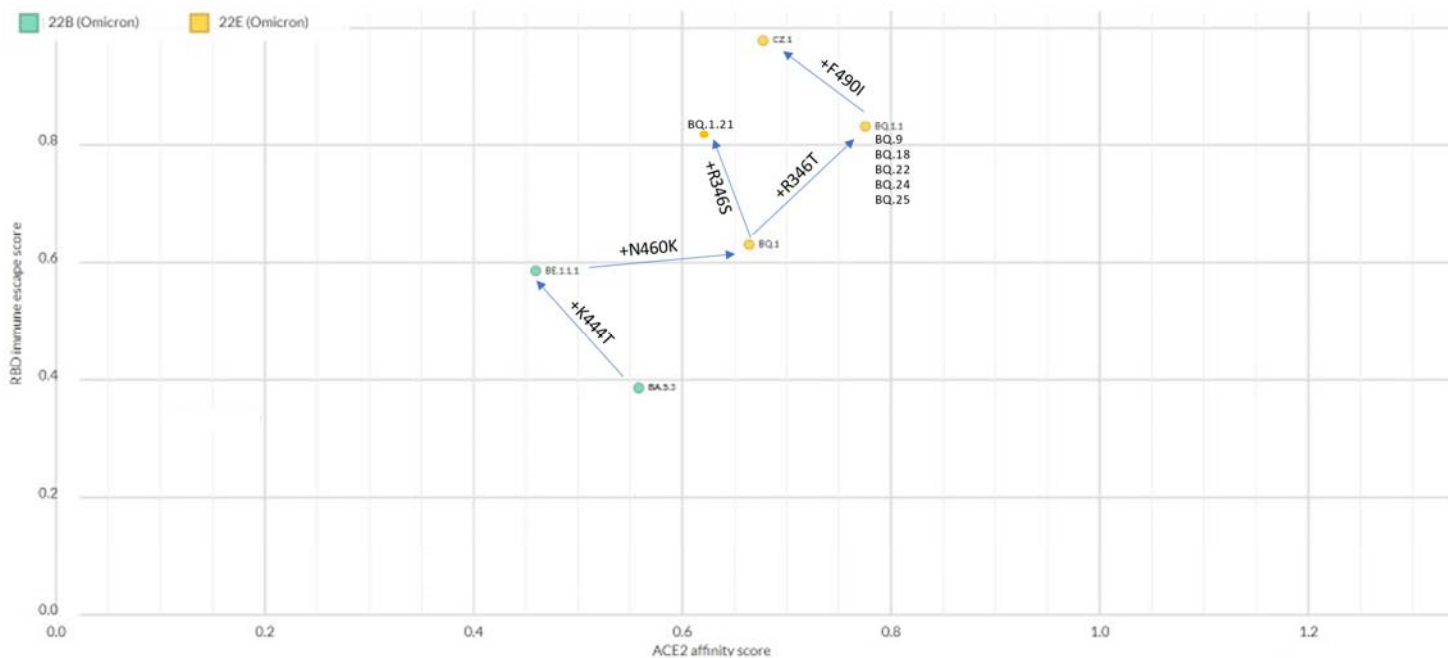
600

### Convergent evolution steps at the origin other BA.2.75.\* branches



601

### Convergent evolution steps in RBD increase immune escape: the CZ.1 case

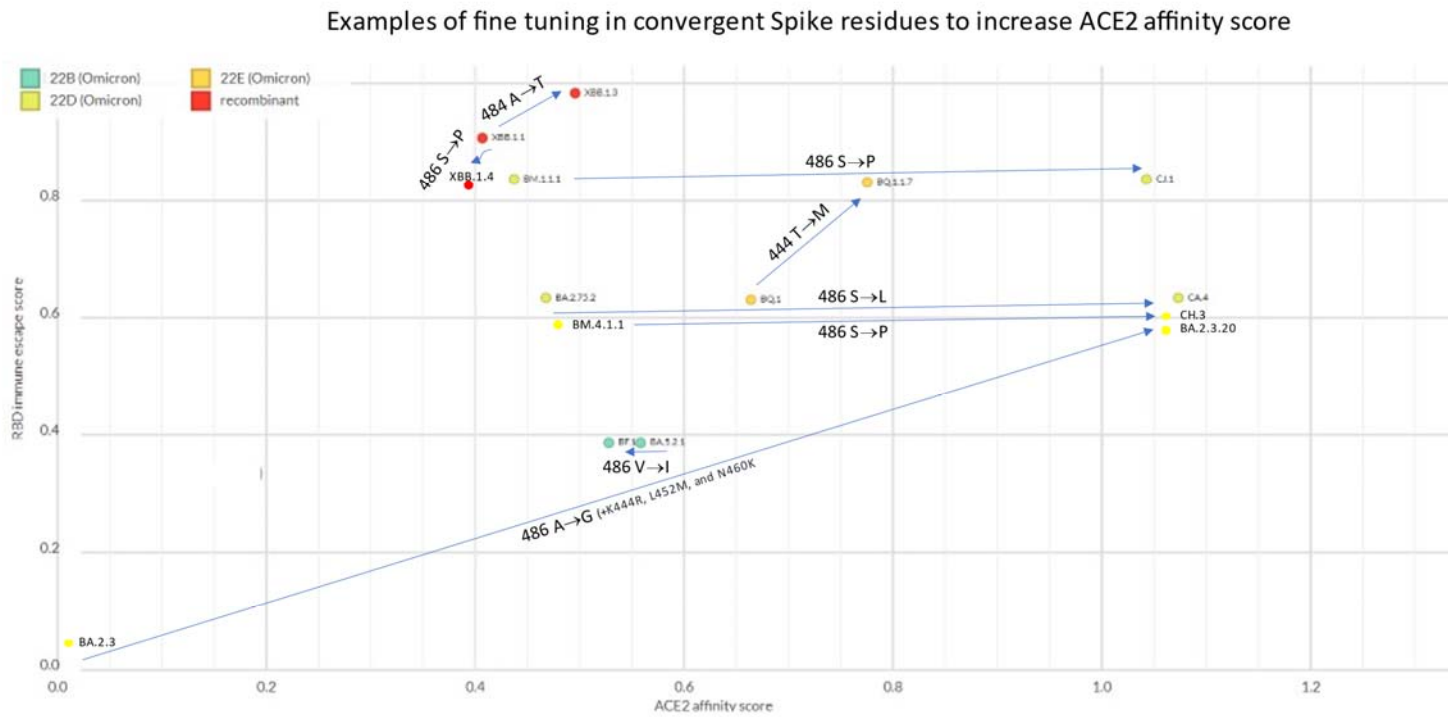




603  
604  
605  
606  
607

## Figure 6

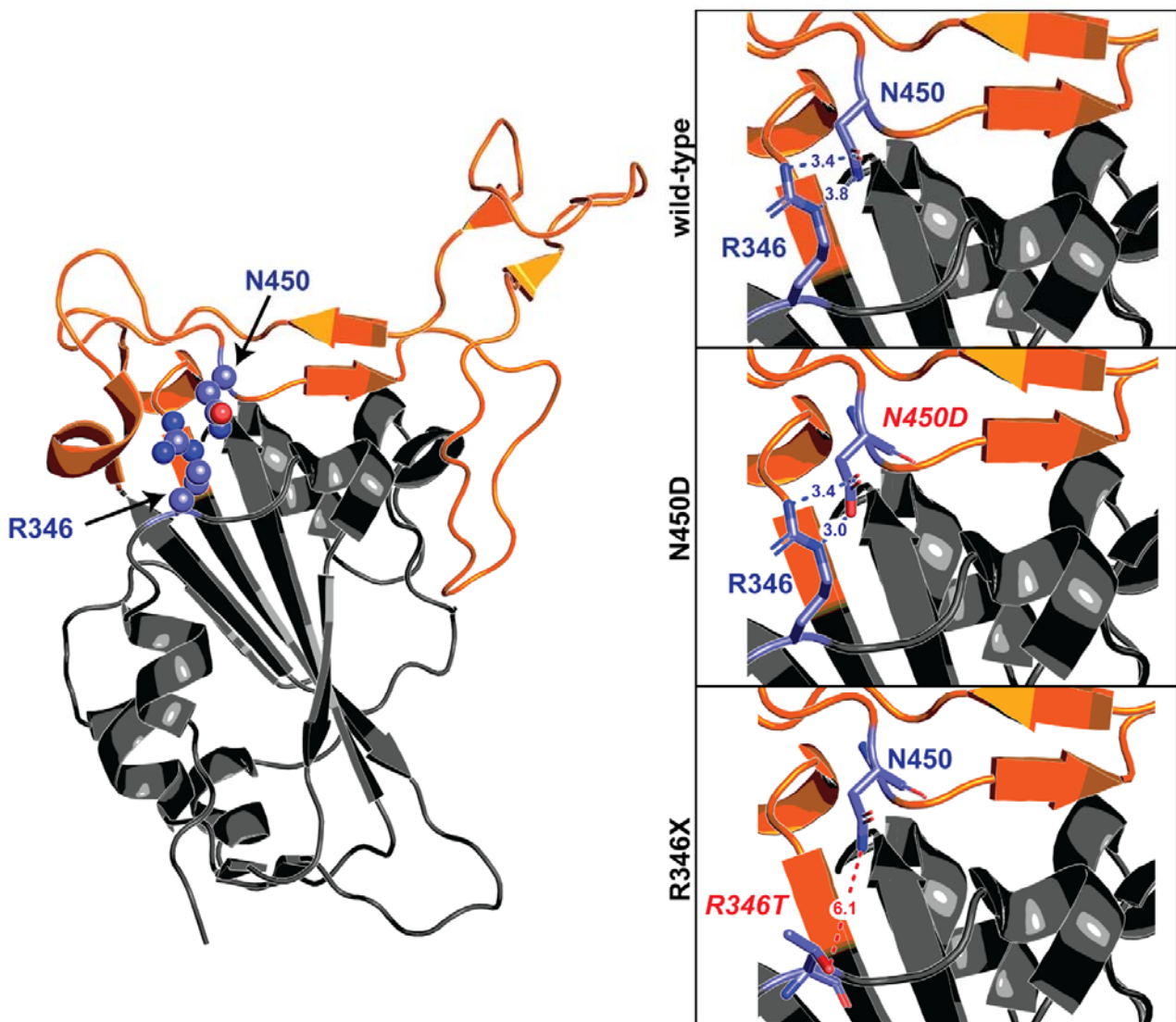
Sequential mutational events at the same Spike amino acid residues showing no change or progressive increases in ACE2 affinity score (as calculated here: [https://github.com/jbloomlab/SARS-CoV-2-RBD\\_DMS\\_Omicron/blob/main/results/final\\_variant\\_scores/final\\_variant\\_scores.csv](https://github.com/jbloomlab/SARS-CoV-2-RBD_DMS_Omicron/blob/main/results/final_variant_scores/final_variant_scores.csv)). Chart created on NextStrain [68] ([https://next.nextstrain.org/staging/nextclade/sars-cov-2/21L?gmin=15&l=scatter&scatterX=ace2\\_binding&scatterY=immune\\_escape&showBranchLabels=all](https://next.nextstrain.org/staging/nextclade/sars-cov-2/21L?gmin=15&l=scatter&scatterX=ace2_binding&scatterY=immune_escape&showBranchLabels=all))



608

609 **Figure 7**

610 Mutually exclusive mutations at R346 and N450. The receptor binding domain of S is depicted in grey cartoon representation, with the receptor binding  
611 module (ACE2 interaction interface) highlighted in orange. Amino acids at the 346 and 450 positions are displayed as purple sticks. A zoomed-in view of the  
612 R346-N450 interaction in the ancestral domain, as well as the computationally modelled amino acid substitutions at those two positions, are portrayed in  
613 boxes to the right. In the wild-type sequence, the basic R346 sidechain interacts with the N450 residue through a pair of hydrogen bond interactions.  
614 N450D results in a similarly sized sidechain, but altered electrostatics. One hydrogen bond is maintained between the neutral oxygen of Asp and Ne of Arg,  
615 and a new salt bridge is formed between the anionic deprotonated oxygen of Asp and the cationic center of the guanidino group of Arg. In the case of  
616 R346X, any substitution except lysine would result in a side chain that is significantly shorter and non-cationic, thus dissolving the interactions between  
617 N450 or other common substitutions at that position.



619

620

621

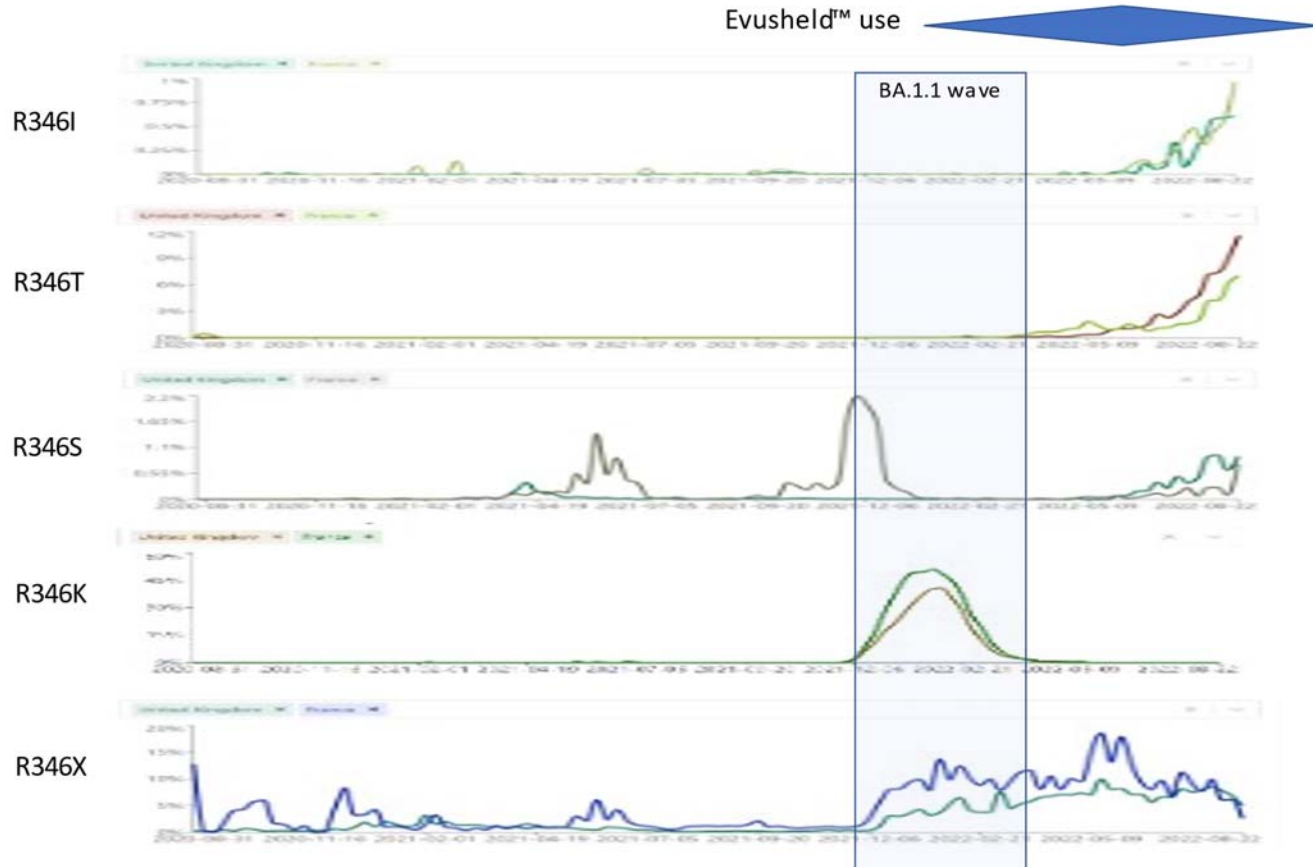
## Figure 8

622

Prevalence of S:R346X mutations in the period 2020-08-27 – 2022-09-13 in UK versus France. Sourced from <https://cov-spectrum.org> on November 26,

623

2022. The blue area represents trends in Evusheld™ prescriptions in France and many other countries (but not UK).



624